SIZE FRACTIONATION OF MAGNETIC NANOPARTICLES BY USING CONTINUOUS FLOW LOW GRADIENT MAGNETIC SEPARATION TECHNIQUE

CHAN WEI JIE

UNIVERSITI TUNKU ABDUL RAHMAN

SIZE FRACTIONATION OF MAGNETIC NANOPARTICLES BY USING CONTINUOUS FLOW LOW GRADIENT MAGNETIC SEPARATION TECHNIQUE

CHAN WEI JIE

**A project report submitted in partial fulfillment of the
requirements for the award of the degree of
Bachelor of Engineering (Honours) Petrochemical Engineering**

**Faculty of Engineering and Green Technology
Universiti Tunku Abdul Rahman**

May 2023

DECLARATION

I hereby declare that this project report is based on my original work except for citations and quotations which have been duly acknowledged. I also declare that it has not been previously and concurrently submitted for any other degree or award at UTAR or other institutions.

Signature : _[signature]_

Name   : **CHAN WEI JIE**

ID No.   : **18AGB04214**

Date   : **29 APRIL 2023**

APPROVAL FOR SUBMISSION

I certify that this project report entitled "**SIZE FRACTIONATION OF MAGNETIC NANOPARTICLES BY USING CONTINUOUS FLOW LOW GRADIENT MAGNETIC SEPARATION TECHNIQUE**" was prepared by **CHAN WEI JIE** has met the required standard for submission in partial fulfilment of the requirements for the award of Bachelor of Engineering (Honours) Petrochemical Engineering at Universiti Tunku Abdul Rahman.

Approved by,

Signature	:	
Supervisor	:	Ir. Ts. Dr. Toh Pey Yi
Date	:	29/4/23

Specially dedicated to

my beloved, father, sister, mother and all my friends.

ACKNOWLEDGEMENTS

I would like to thank everyone who had contributed to the successful completion of this project. I would like to express my gratitude to my research supervisor, Dr Toh Pey Yi and Dr. Leong Sim Siong for their invaluable advice, guidance, and enormous patience throughout the development of the research.

In addition, I would also like to express my gratitude to my loving parents and friends who had helped and given me encouragement along the research period

SIZE FRACTIONATION OF MAGNETIC NANOPARTICLES BY USING CONTINUOUS FLOW LOW GRADIENT MAGNETIC SEPARATION TECHNIQUE

ABSTRACT

Colloidal instability has prevented widespread usage of magnetic nanoparticles (MNPs) in a variety of engineering applications. The colloidal stability of MNPs can be enhanced by surface modification or functionalization with polyelectrolytes, however it is still difficult to determine the ideal functionalization conditions for generating the most stable MNP systems. This research overcomes this obstacle by examining the average particle size and particle size distribution of MNP systems produced by altering the mass ratio of polyelectrolyte (PSS) to MNPs during surface functionalization. According to the results, the lowest average hydrodynamic size and narrowest particle size distribution were achieved in an MNP system where the mass ratio of MNPs to polyelectrolyte (PSS) was 1:1. Also, the study presented the Continuous-Flow Low-Gradient Magnetic Separation (CF-LGMS) method of making MNPs with enhanced monodispersity. This investigation conducted an experimental investigation into how flowrate and magnet configurations affect the monodispersity of CF-LGMS-fractionated systems of magnetic nanoparticles. The results demonstrated that the size fractionation of MNPs via the CF-LGMS process was greatly enhanced by a slower flowrate (5 ml/min) and a higher quantity of magnets (dual pair magnet arrangement), resulting in a monodispersed MNP system. Eventually, the study used COMSOL Multiphysics to create a mathematical model of the CF-LGMS fractionation process. The model's ability to predict and optimise the performance of the CF-LGMS process was demonstrated by the high degree of agreement between the simulated and experimental findings. Many engineering applications, including as MRI, drug administration, and magnetic hyperthermia, rely

on MNPs with high colloidal stability and monodispersity, and this work contributes to that knowledge.

TABLE OF CONTENTS

LIST OF TABLES

\

LIST OF FIGURES

LIST OF SYMBOLS / ABBREVIATIONS

∇B   Magnetic field gradient, T/m

T   Magnetic field flux density, T

N^* Aggregation parameter

D_{cr} Critical size for monodomain, nm

D_{sp} Critical size for superparamagnetic behavior, nm

F_{mag} Magnetophoretic force, N

μ   Magnetic dipole moment, $A \cdot m^2$

M   Magnetization, A/m

V   Volume of MNPs, m^3

d   Core diameter of MNPs, m

r   Radius of MNPs, m

F_d Viscous force, N

η   Viscosity of the suspension, $Pa \cdot s$

d_H Hydrodynamic diameter of MNPs, m

v Magnetophoretic velocity of MNPs, m/s

F_g Gravitational force, N

m   Mass of MNPs, kg

g   Gravitational acceleration, m/s^2

F_b Buoyant force, N

ρ_f Density of fluid, kg/m^3

c   Concentration of MNPs, mgL^{-1}

D   Diffusivity of MNPs, m^2/s

t   Duration of magnetophoresis, s

U_{dd} Dipole-dipole interaction energy, J

μ_o Magnetic permeability of free space, N/A^2

θ Angle between the direction of the external magnetic field and the line joining the centers of the two particles, rad

Γ Magnetic coupling parameter

k_B Boltzmann constant, J/K

T   Temperature, ℃

M_s Saturation magnetization, J/K

Φ_0 Volume fraction of MNPs in the solution

Gr_m Grashof number

ρ Density of MNPs solution, kg/m^3

c_s MNPs concentration at the collection plane, mg/L

$c\infty$ Bulk concentration of MNPs, mg/L

L_c Characteristic length of the system subjected to magnetophoresis, m

υ Kinematic viscosity of the solution, m^2/s

σ Standard deviation, nm

CF-LGMS   Continuous flow low gradient magnetic separation

HGMS   High gradient magnetic separation

LGMS	Low gradient magnetic separation
IONPs	Iron oxide nanoparticles
MNPs	Magnetic nanoparticles
NPs	Nanoparticles
PSS	Poly(sodium 4-styrene sulfonate)
SD	Standard deviation
PDI	Polydispersity index
DLS	Dynamic light scattering

CHAPTER 1

INTRODUCTION

1.1 Magnetic Nanoparticles

Nanotechnology is the study of microscopic material that lies under the comparatively new scientific and technological topic. This microscopic material is also known as nanoparticle (NP) which has one or more than one dimension falls within the range of 0.1 nm to 100 nm. A wide variety of nanoscale materials has been produced as a result of the extensive exploration and research activities. Due to the fact that they are not simple molecules, NPs made of up to three layers. First and foremost, the inner layer is the core material which basically fills up the center region of the NP. This is the most important layer that must be possessed by all NPs. Beyond the core region is the shell layer and this is chemically distinct material from the core in all regards. For example, the shell layer can be the oxide of the core material that encompasses the inner layer of NPs. Outermost layer is the surface layer. This layer could be a range of polymer, surfactants, small molecules and polymer and metal ions that is functionalized with the NP (Khan, Saeed and Khan, 2019).

With the application of nanotechnology and NP, researchers in the life sciences and healthcare are now able to make significant advancements at the cellular and molecular levels. Due to its distinct size and physicochemical characteristics, NP provides many benefits if it is employed in engineering and industrial applications. In comparison to the macroscopic objects, they are very small, and display features that are not seen in bigger structures. However, if compared to atoms and molecules, they are relatively much bigger in size for the quantum phenomena to be effective

(Akbarzadeh, Samiei and Davaran, 2012). Within the size range, NP demonstrates very distinctive properties as compared to its bulk counterpart as well as the atoms/molecules that make up of it.

Based on their physicochemical characteristics, NP can be subdivided into many groups. One of the famous groups of NP is the magnetic nanoparticles (MNPs), which are made of materials that are magnetically responsive. Owing to this reason, the motion of MNPs can be controlled by magnetic fields is the MNP. These particles typically have two parts: (i) functional chemical component (the non-magnetic material deposited on the surface of the particle's core) and (ii) magnetic component (the particle core which is frequently made of iron, nickel, or cobalt).

Despite the fact that bare MNPs are usually colliodally stable on their own, coating with a tiny organic molecule or polymers can stop MNPs from clumping together upon their dispersion in the solution (Hinge et al., 2020). Apart from that, there are some astonishing novel phenomena that are exhibited by MNPs such as high saturation field, superparamagnetic, high field irreversibility, additional anisotropy contributions, and shifted loops after field cooling. These characteristics are resulted from surface and finite size effects due to their tiny dimension, which influence the individual MNP physiochemical behavior (Akbarzadeh, Samiei and Davaran, 2012).

One of the most important features demonstrated by MNP is the superparamagnetism, which can be found in the particles that are smaller than a critical size (superparamagnetic limit). Superparamagnetic material is displaying the attractive feature from both ferromagnetic and paramagnetic materials. Here, MNP (with superparamagnetic characteristic) has a strong saturation magnetization (as displayed by the ferromagnetic material) and no magnetic memory (as displayed by the paramagnetic material). As shown in Figure 1.1, superparamagnetic material will gain magnetization under magnetic field and achieve very high saturation magnetization as shown by ferromagnetic material, however, the magnetization is completely lost once the magnetic field is removed.
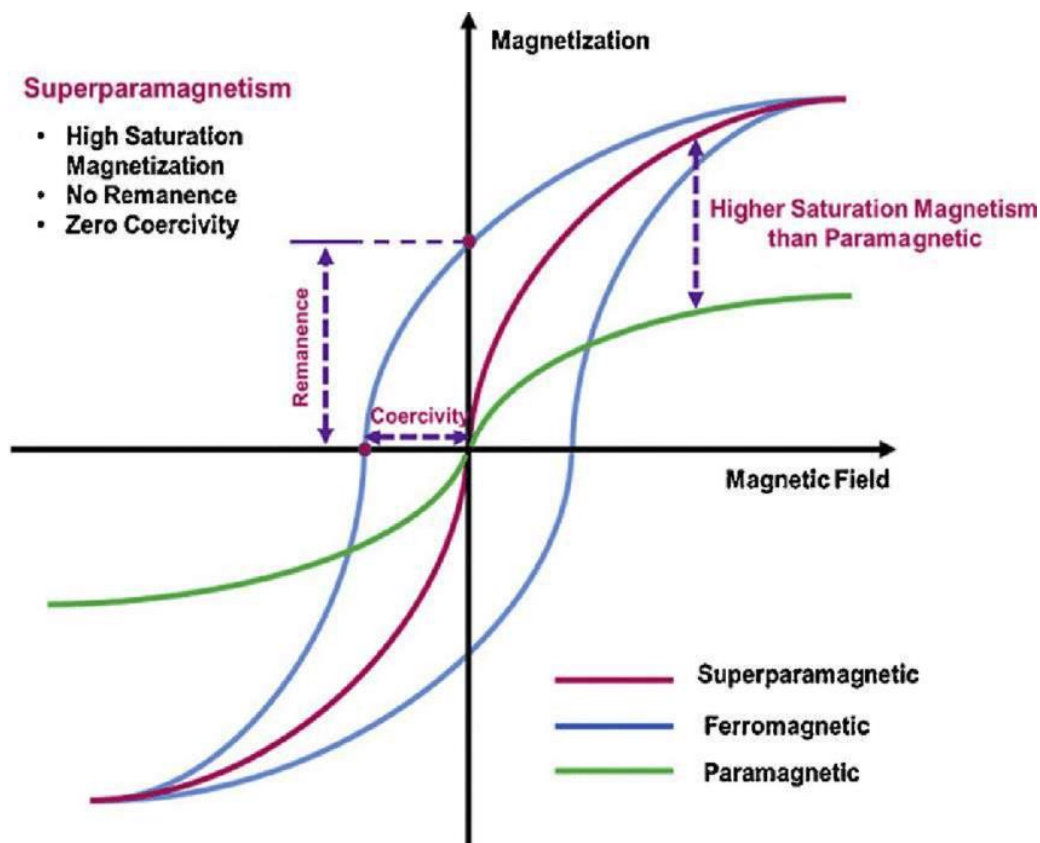
Figure 1.1: Hysteresis loop of Superparamagnetic, Ferromagnetic and Paramagnetic Materials (Gatard, 2021).

On the other hand, MNPs have another vital feature which is the high surface to volume ratio, which means that a disproportionately large number of their molecules or atoms are exposed on their surface. With decreasing particle size, this ratio becomes more important, leading to a greater relative surface area for tiny nanoparticles. NP' superior ability to interact with their surroundings due to their high surface to volume ratio is crucial. For instance, medication delivery, biosensors, and magnetic separation can all benefit from MNPs having a high surface-to-volume ratio because more functional groups can be added to their surface. MNPs may be advantageous for magnetic data storage and other applications due to the enhanced magnetic characteristics that can emerge from the enhanced magnetic interactions made possible by their large surface area.

MNPs are frequently employed in biological applications because of their flexibility to be tailored to possess bio-compactness characteristics. Analytical and therapeutic applications are the two primary uses of MNPs in the field of biomedicine. MNPs are utilised in analytical applications as contrast agents for imaging, magnetic resonance as well as magnetic carriers in separation processes, and molecular recognition events biosensors. The utilisation of MNPs for medication transport into cells and for hyperthermia during cancer treatment are two of its main therapeutic uses (Tartaj et al., 2016). Their high surface area to volume ratio is what makes them suitable for certain applications. Due to their ease of interacting with biomolecules such as proteins, enzymes, antibodies, and nucleotides, MNPs have become essential for in vivo medicinal reasons. In vivo biomedical applications require MNPs with desirable properties, including high saturation magnetization, small particle size, regular shape, and biocompatible and biodegradable surface functionalization.. By controlling the synthesis processes and the substances utilised for surface functionalization, MNPs may be compared to biological creatures made up of cells, genes, proteins, and viruses (Aisida, Ahmad and Ezema, 2022). Moreover, magnetic nanoparticles also can be utilized in wastewater treatment system. The functionalized MNPs are often introduced to an untreated solution as part of a separation process in order to selectively attach the desired contaminants to the MNPs. The MNPs and the attached impurities are then drawn to a magnet, drawing them out of the solution (Chong et al., 2021).

1.2   Magnetophoresis of MNPs under Continuous Flow Mode

The movement of MNPs in relation to their surrounding fluid when a gradient of magnetic field is applied externally is known as magnetophoresis. One of the main advantages of this MNP-based water treatment method is the recollection ability of MNPs, which may be readily done using a portable permanent magnet once the harmful chemical has been adsorbed onto the particle surfaces. This separation approach has a simple fundamental idea. Its basic premise is that magnetic particles undergo magnetophoresis in the presence of magnetic field gradients, and that a

magnetic source will physically separate these materials from the surrounding fluids (Lim, Yeap and Low, 2014).

Magnetic separation of MNPs by using magnetohoresis is further classified into two types which are high gradient magnetic separation (HGMS) and low gradient magnetic separation (LGMS). HGMS is a continuous flow technique that separates MNPs from a liquid suspension under a high magnetic field gradient ($\nabla B \geq 100$ T/m) that can only be created by an electromagnet generated by great electrical power. A general HGMS column comprises of a magnetizable wire coil situated in the center of the separation column to generate disruptions into the magnetic field, resulting in a considerably greater and localized magnetic field gradient on certain areas of the wire coil. The high magnetic field gradient is able to impose sufficiently large magnetophoresis on MNPs and induces the rapid separation of MNPs from their suspension. However, HGMS required enormous amount of energy supply to generate the high magnetic field gradient. Thus, the cost will be increased as well. Additionally, there is a chance of adhesion of MNPs or other contaminants on the surface electromagnet wires which will decrease the separation efficiency.

On the other hand, LGMS, is performed under the absence of the magnetizable wire, hence, only low magnetic field gradient ($\nabla B < 100$T/m), can be produced across the MNP solution by using just a handheld permanent magnet. Such an operational setup has considerably simplified the internal design of the magnetic separator. Despite of the low magnetic field gradient and magnetic force imposed on individual MNPs under LGMS scheme, the separation of MNPs still can be accomplished relatively fast. This phenomenon is attributed to the two interactions that occurs during the magnetophoresis of MNPs. The first interaction is particle-particle interaction from the magnetic dipole moment own by them. In this context, the self-aggregation of MNPs (due to the attraction between the magnetized MNPs) will take place during the magnetophoresis, which will lead to the development of larger MNP aggregated with the higher velocities than individual MNPs. Therefore, this phenomenon is called the cooperative effect of magnetophoresis. It is crystal clear that this cooperative effect highly depends on the MNPs' concentration inside the solution. When the concentration of MNPs increases, the extent of MNP interaction and self-aggregation is higher, which resulting in the creation of aggregates which move at greater velocity

(Faraudo, Andreu and Camacho, 2013). In addition, particle-fluid interaction (momentum transfer between MNPs and fluid) also improves the separation rate of MNPs subjected to LGMS. With the particle-fluid interaction, the non-magnetic surrounding fluid also can gain momentum and flow convectively, which gives rise to magnetophoresis. The inhomogeneity of the magnetophoretic force imparted on the whole solution may be seen as the macroscopic cause of the induced convection that is generated across the MNP solution during magnetophoresis. Based on the experiment done by various researchers, throughout the duration of magnetophoresis, there is no discernible change in the concentration of the MNP solution. (in which the hydrodynamic effect is dominating), but the overall concentration still decreases due to the continuous depletion of MNPs. The illustration of cooperative and hydrodynamic effects, which govern the transport behavior of MNPs during magnetophoresis process, are shown in **Figure 1.2** (Leong et al., 2020).
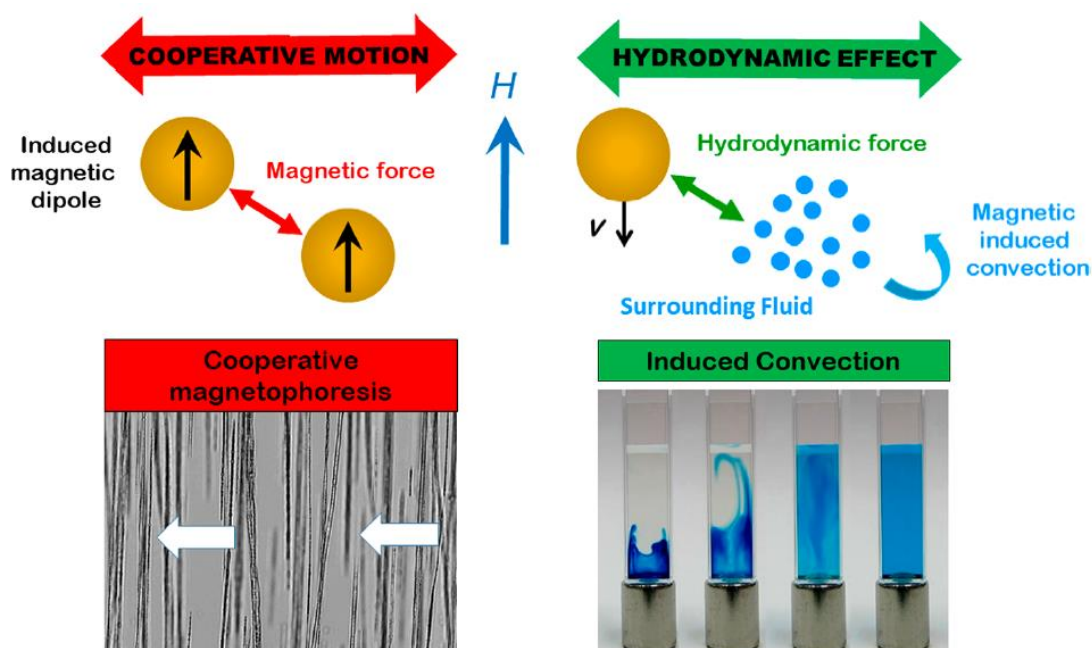
Figure 1.2: Cooperative and Hydrodynamics Effects during Magnetophoresis (Leong et al., 2020).

Yet, most of the studies related to LGMS are conducted in the batchwise method and lab-scaled container, which is not appropriate to be directly employed in large scale industrial applications. However, it would be appealing to create a low

gradient magnetic field separator that operates in a continuous flow method, since this would make the LGMS technology to be easier applied in industrial settings. With the help of the continuous flow low gradient magnetic separator (CF-LGMS), the MNP solution could constantly flow through the separation column, allowing the simultaneous separation of MNPs from their original suspension without the need of extensive labor force (Chong et al., 2021). In addition, the integration of continuous flow features of LGMS also can facilitate the process control and automation. **Figure 1.3** shows the concept diagram of CF-LGMS, in which the solution containing MNPs will enter the separator through the inlet and being separated from the solution within the separator, by the magnets located at the surroundings, and leaving out the clean solution free of MNPs at the outlet.
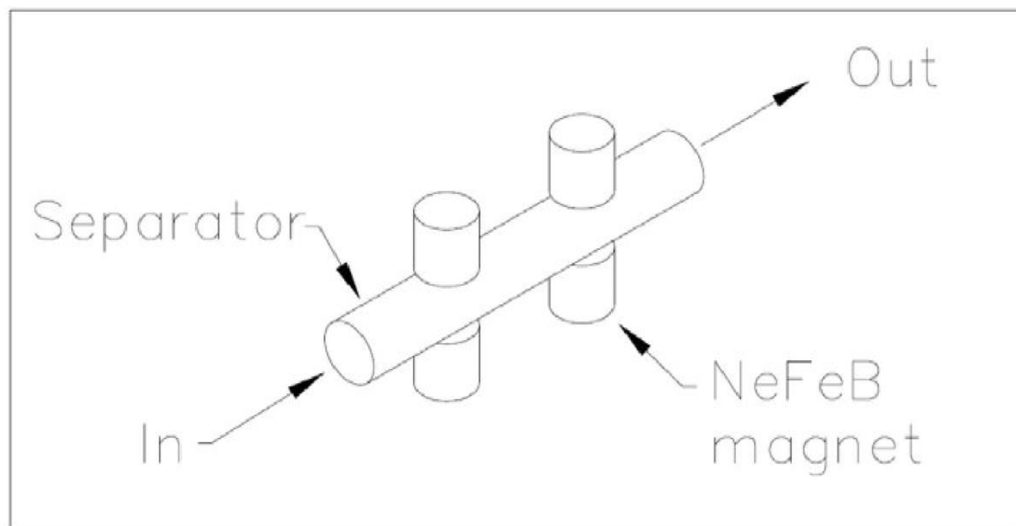
Figure 1.3: Sample of Separator for CF-LGMS (Chong et al., 2021).

1.3   Problem Statement

The MNPs are excellent for biomedical applications because they are easily stabilised under physiological circumstances and are not prone to significant magnetic interactions during dispersion. In spite of that, according to conventional perspective, MNPs used in cancer therapy should have a size between 5 and 100 nm, where the blood circulation time and enhanced permeability and retention (EPR) effects are maximised. When the particle size is too large, it is easily retained by cells in the

reticuloendothelial system (RES) organs, whereas when it is too tiny, it can be quickly eliminated through the kidneys (Feng et al., 2018). Besides that, in order to ensure the safety and effectiveness of drug delivery of MNPs, the size of MNPs must be as small as possible. The tiny size of MNPs also can enhance the tissular diffusion of the particles, significantly effective surface areas as well as long sedimentation period during the drug delivery. But, too small of size in MNPs will lead to other toxicity issues (Tartaj et al., 2016). Since regulated biodistribution, bioelimination, and contrast effects depend on each nanoparticle having essentially identical physical and chemical characteristics, monodisperse magnetic nanoparticles are necessary for many prospective biomedical uses (Xu and Sun, 2007). Therefore, it is vital to control the particle size within the provided range and high monodispersity of MNPs is desired.

However, in order to obtain a MNP system with great extent of monodispersity, certain highly expensive/rigorous techniques must be used. For instance, monodispersed MNPs with a relatively narrow size distribution could be produced by thermal decomposition, polyol, laser pyrolysis, spray pyrolysis and microemulsion. These procedures may include the use of hazardous or poisonous materials, high temperatures, stringent working conditions, complicated synthesis process and long period of synthesis(Ajinkya et al., 2020). On the other hand, the relatively less expensive and less rigorous method for MNP synthesis, such as co-precipiation of iron precursor can result in MNP systems with substantial degree of polydispersity. In addition, the colloidal stability of MNPs is also a great concern when they are being dispersed in the solution. As the aggregation and process is spontaneously in nature, unmodified MNPs can be subjected to severe aggregation and produce aggregates of very different size which leading to the formation of highly polydispersed MNP system. Even though, the surface functionalization (or coating) of MNP with macromolecules can improve the colloidal stability, the resulted MNP-macromolecule clusters can show huge deviation in size and might be unsuitable for some applications which have high requirement on the degree of monodispersity of MNP system. As a result, it is crucial to look for a simple and low-cost strategy to produce the MNP system with improved degree of monodispersity, which is the major intention of this project.

In the year of 2014, there was a study being conducted to perform the size fraction of polyelectrolyte-functionalzed MNP clusters, with high degree of polydispersity, by using LGMS technique (Yeap et al., 2014). The size fractionation of MNPs is principally due to the fact that the larger MNP cluster can be driven to move relatively faster and separated more rapidly from the solution, as compared to its smaller counterpart. Therefore, the first MNP fraction obtained (or captured by the LGMS system) is having the largest size and the subsequent fractions consists of MNP clusters with smaller size. By this way, the MNPs are segregated according to the size and each fraction will possess the lower extent of polydispersity as compared to the original MNP solution. As MNP solution must be manually inserted; however, when using a continuous flow method, a pump is used to automatically inject the MNP solution. During the continuous flow separation of MNPs, the larger or aggregated MNPs would have greater velocities as compared to the single or tiny MNPs. This is mainly due to the larger particles that tend to experience more magnetophoretic separation (Yeap et al., 2014).

Despite being more readily available and less expensive to create, the received functionalized MNPs are frequently particularly polydisperse due to the uncontrolled aggregation of MNPs. Therefore, adopting the magnetophoresis approach to fractionate the polydispersed MNP system into comparatively monodispersed MNP systems might be quite attractive. In this study, the size fractionation of the MNP system with high polydispersity is carried out using continuous flow low gradient magnetic separation. Therefore, size fractionation of MNPs during continuous flow of magnetophoresis can be achieved and this separation depending on the MNPs concentration, retention time and flow rate.

1.4   Research Objectives

- To prepared functionalized magnetic nanoparticles by using polyelectrolyte grafting technique.
- To experimentally study the effect of flowrate and magnet configurations on the monodispersity of magnetic nanoparticle systems fractionated by continuous flow low gradient magnetic separation technique.
- To develop a mathematical model which is able to describe the fractionation process by using continuous flow low gradient magnetic separation technique.

CHAPTER 2

LITERATURE REVIEW

2.1 Magnetic Nanoparticles (MNPs)

Current developments in nanotechnology field have led to the advancement and revolution of a variety of industries. The application of nanotechnology in various engineering sectors is expanding rapidly. One of the elements that play a crucial role in nanotechnology is nanoparticles. Nanoparticles (NPs) are tiny particles with typical sizes between 1 and 100 nm, which set them apart from their bulky parent materials and make them equip with unique characteristics for a variety of applications. Magnetic nanoparticles (MNPs), a nanoscale substance with specific magnetic characteristics, are one of the special class of NPs and have been extensively employed in various field, including biomedical, energy, engineering, and environmental applications. Due to the distinct features and magnetic properties exhibited by the MNPs, they have been widely used in biomedicine, catalysis, agriculture, and environment sectors. So, they have recently attracted the attention of many researchers from the worldwide to study them, such as identifying a better way to synthesize MNPs with the better characteristics, exploring their potential usage for the advancement of human's technology, improving their performance as well as efficiency of them in existing applications and etc. The combination of different metal elements (either alone or in composites) and their oxides with magnetic behavior at nanoscale can give rise to MNPs. The most often utilized MNPs are made of iron (II,III) oxide which is also known as magnetite (Fe_3O_4) because of its superparamagnetic behavior, great biocompatibility and low toxicity. In this regard, the development and

understanding of iron oxide MNPs' potential applications in several fields has recently attracted a lot of interest.

The domains in ferromagnetic or ferrimagnetic materials' macroscopic crystals have well-defined sizes and magnetizations, and they are isolated from one another via domain walls. Such a multidomain sample's magnetization is altered by domain wall displacements when a magnetic field is present. Each material has a different characteristic minimum size D_{cr} for these domains. Particles that are smaller than this minimum size (usually below 100 nm) often only have one magnetic domain, they retain their uniform magnetization even when exposed to no external magnetic field. **Figure 2.1** illustrates how the size of magnetic particles affects their behavior. A change in magnetization caused by an external field requires rotation of the entire particle's magnetic moment since domain wall displacement is impossible in a single domain particle. When the size of nanoparticles is very small, it will reach a superparamagnetic state. Magnetic moment measurements will always result in zero in the absence of an applied field due to the rapidity with which the nanocrystal's MNPs spontaneously flip to the superparamagnetic state. Therefore, in the presence of an applied field, the particles behave like a paramagnetic substance with a strong saturation magnetization, stabilizing their dipole in the direction of the field (Leong et al., 2020).
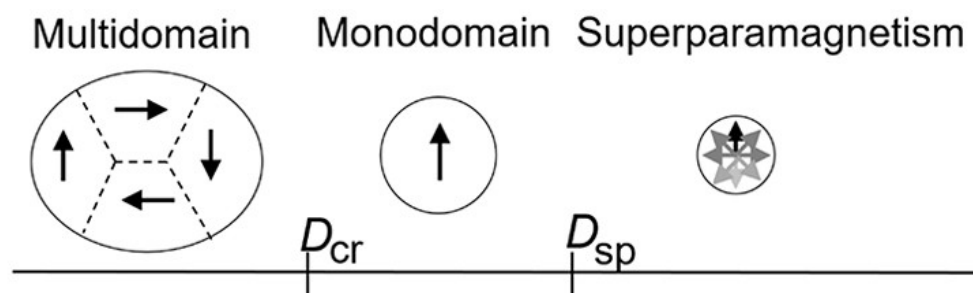
Figure 2.1: Diagram showing how the size of magnetic particles affects their behavior. D_{sp} stands for the critical size for superparamagnetic behavior, whereas D_{cr} stands for the critical size for monodomain behavior (Leong et al., 2020).

2.1.1   Synthesis method and size distribution of the resulted MNPs

There are various ways to produce MNPs for various applications such as co-precipitation, thermal decomposition, microemulsion, hydrothermal and polyol. Co-precipitation technique is a simple way to create Fe_3O_4 with a success rate between 96 and 99.9 percent. This approach uses an alkaline medium with a ferrous to ferric ions ratio of 1:2. Microscopic, stoichiometric of single and multi-component metal oxides metal oxide particles can be generated via chemical co-precipitation (Koo et al., 2019). There is further work to be done to simplify and improve upon the co-precipitation approach for synthesizing magnetite particles with high dispersion and narrow size distribution. The production method is crucial to ensuring that magnetite nanoparticles have consistent physical and chemical properties. The convenient co-precipitation method will produce poor morphology and particle size distribution due to the growth of the MNP crystal is usually conducted under an uncontrolled environment. The improved co-precipitation approach can be enhanced by employing an organic combination of A1416 and kerosene as a stabilizing agent to regulate the nucleation process, hence controlling particle size distribution and improving dispersion. However,   this synthesis process does not employ aqueous solution, and the resulted MNPs need to be transferred to the aqueous solution if they are to be used in aqueous environment (the common application environment of MNPs), which imposes additional step and may brought about particle aggregation during the transfer (Wang, Wei and Qu, 2013).

On the other hand, thermal decomposition of organometallic compounds $Fe(cup)_3$(cup = N-nitrosophenylhydroxylamine), $Fe(acac)_3$(acac = acetylacetonate), or $Fe(CO)_5$ and followed by oxidation is another MNP synthesis method that is able to produce monodispersed MNPs with high quality (Wu, He and Jiang, 2008). According to Sun and Zeng, the typical decomposition method is according to the elevated temperature (265 °C) to induce the reaction of $Fe(acac)_3$ in phenyl ether under the presence of oleylamine, alcohol and oleic acid to produce size controlled monodispersed MNPs. Seed-mediated growth allows for the production and dispersion in a nonpolar solvent of larger monodispersed magnetite NPs with diameters of up to 20 nm, utilizing the smaller magnetite NPs as the starting material. The approach does not need size selection and it could be easily scaled up for mass

manufacturing. It is possible to easily transform the produced Fe_3O_4 nanoparticle assemblies into Fe_2O_3 NPs by treating them at high temperature (250 °C) and oxygen for 2 hours. Even though the thermal decomposition process has significant pros for generating remarkably monodispersed particles that exhibit a narrow size distribution, but the synthesis process is typically conducted in nonpolar liquids which imposes an additional step to transfer the synthesized MNPs to the aqueous medium in many applications (Wu, He and Jiang, 2008). In addition, the chemicals involved in this synthesis method are relatively expensive as compared to those being used in the MNP synthesis by co-precipitation method.

The microemulsion technique can also be used to produce MNPs. Microemulsions are a type of surfactant-stabilized emulsion in which two otherwise incompatible liquids are mixed together to form a monolayer with negligible interfacial tension. In this method, MNPs are generally created in microemulsions by intramicellar nucleation and growth. The nano-sized water droplets in a continuous oil medium that make up a microemulsion are held in place by molecules of surfactant and cosurfactant, making the system thermodynamically stable. Because the water droplets act as nanoreactors while the metal precursors are dissolved in them, the resulting particles are uniform and easy to handle (Salvador et al., 2021). The choice of the surfactant has a significant impact on the physicochemical characteristics of NPs produced with this method. In general, nanoparticles synthesized by this method have a nearly monodisperse spherical form with an average diameter between 10 and 25 nm (Ansari et al., 2019). Vidal-Vidal et al. claim that spherical particles with a monolayer covering of oleylamine (or oleic acid) may be produced by the production of monodisperse maghemite NPs using the one-pot microemulsion process. They are highly magnetized and crystalline, with a size distribution of 3.5 ± 0.6 nm. (Vidal-Vidal, Rivas and López-Quintela, 2006). Although surfactants are present, the aggregation of the synthesized NPs still can occur after the multiple washing operations (to remove one of the immiscible liquids and disperse the MNPs into aqueous medium) and further stabilizing treatments might be required (Wu, He and Jiang, 2008).

Magnetic nanoparticle (MNP) characteristics depend critically on both size and shape, thus, it is vital to produce MNPs with these controlled parameters. The MNP

synthesis method as mentioned above (thermal decomposition and microemulsion) basically resulted in complicated process or required elevated temperatures. Another option is hydrothermal synthesis, which employs a number of wet-chemical techniques to crystallize substances in a sealed container at high vapor pressure and temperature (typically between 0.3 and 4 MPa and 130-250 °C) (Wu, He and Jiang, 2008). Hydrothermal reduction was proposed by Li et al. to create microspheres of monodisperse, hydrophilic, single crystalline ferrite. A clear solution was obtained by adding $FeCl_3$ to a mixture containing ethylene glycol, sodium acetate, and polyethylene glycol, and then vigorously stirring the contents. The mixture was then placed in an autoclave, which is a stainless steel container with a Teflon lining, and heated to and maintained at 200 °C for 8 to 72 hours. This method yielded monodisperse ferrite spheres with sizes ranging from 200 to 800 nm. (Lu, Salabas and Schüth, 2007).

Apart from that, polyol method is also another route to produce MNPs. The polyol approach to synthesis MNPs is conducted on the basis of the precursor substances including oxides, acetates, and nitrates that are dissolved or suspended in diols. This enables the synthesis of MNPs with consistent physical properties at a relatively low temperature. This technology is adaptable and may be scaled to accommodate high volumes of IONP manufacture. The nature of the polyol solvent or the organometallic precursors, as well as the reaction circumstances (such as temperature, reaction time, heating profile, etc.), it can produce spherical MNPs as small as 4 nm in diameter or as large as 100 nm. The polyol method may be used to create nanocrystalline alloys and bio-metallic clusters (Ansari et al., 2019). **Table 2.1** shows the of summary comparison of the synthesis method.

Table 2.1: Summary comparison of the synthesis methods (Ajinkya et al., 2022 & Lu, Salabas and Schüth, 2007)

Synthesis Method	Reaction temperature (°C)	Reaction period	Size distribution	Pros	Cons
Co-precipitation	20-90	Minutes	Relatively narrow	Simple process, quick and easy technique of preparation, and simple control of particle size and composition	Significant aggregation, poor morphology, and unequal distribution of particle sizes
Thermal decomposition	100-320	Hours-day	Very narrow	Generating particles with a narrow size distribution that are highly monodispersed	Expensive, time-consuming synthesis procedure, and high temperature
Microemulsion	20-50	Hours	Narrow	Possible to create monodispersed nanoparticles with diverse morphologies	Ineffective and difficult to scale up

Hydrothermal synthesis	220	Hours-days	Very narrow	Generating particles with a narrow size distribution that are highly monodispersed	Required high temperature and pressure
Polyol	130-220	hours	Relatively narrow	It is possible to make uniform-sized particles and to scale them up.	Takes a lot of time and a high temperature.

2.1.2   Application of MNPs

In recent years, MNPs have been employed in many applications. For instance, MNPs have been used in various industries such as wastewater treatment system, sensing, energy storage, pollution prevention, biomedical field, construction as well as electronics. This section emphasizes on the application of MNPs in wastewater treatment and biomedical fields, which are the two areas that are closely relevant to the application of MNPs in chemical engineering.

2.1.2(a)   Wastewater Treatment

MNPs demonstrate high potential in wastewater treatment due to several appealing features such as elements are low cost, environmentally friendly, high sustainability, high reusability of treatment materials as well as flexible and effective (Zhang and Fang, 2010). Such appealing features displayed by MNPs is owing to the special physical characteristic possessed by them, which are high surface area to volume ratio and intrinsic magnetic property. For instance, due to their tiny size, MNPs have extremely huge surface area for adsorption and reaction purposes, which causes them to have high efficiency in performing adsorption and catalytic activities. Thus, only a trivial amount of MNP material is required to perform the adsorption or catalytic function. In addition, MNPs can be remotely manipulated by external magnetic fields in non-contact mode due to the intrinsic magnetic properties that they possessTherefore, MNPs and magnetic separation are often used together in adsorption processes for water purification and restoration of the environment (Ambashta and Sillanpää, 2010).

MNPs especially iron oxide are favorable in industrial scale wastewater treatment because of their easy separation, adsorption ability, enhanced stability as well as low cost. Usually, the function of MNPs in wastewater treatment system can be separated into two major types: (i) Due to their high surface area, MNPs can serve as a nanosorbent or immobilization carrier to boost removal efficiency (there is only physical adsorption occurring and no chemical reaction incurred in this case); and (ii)

MNPs can play a role as photocatalysts to break down or transform pollutants into a less hazardous formunder the presence of sunlight (chemical reaction is taking place in this case).

In particular, iron oxide magnetic NMs appear to be one of the most promising materials for treating wastewater with high heavy metals content. For example, it has been discovered that surface-modified MNPs are helpful for removing a variety of trace heavy metals from aqueous solutions, including selenium, chromium, lead, uranium, mercury, lanthanide, copper, iron, and cadmium. Nassar's (2010) research found that compared to previously published low cost adsorbents, Fe_3O_4 nanoparticles exhibited a much higher maximum adsorption capacity for Pb(II) ions, at 36.0 mg/g. Because of the nanoscale nature of Fe_3O_4 nanosorbents, metal ions were able to more easily migrate from solution onto the surface's active sites. In addition, throughout the studies, there is no noticeable decline in the adsorption capacity of Fe_3O_4 nanoadsorbents after several cycles of operation. Evidently, the Fe_3O_4 nanoadsorbents can be employed to recover and remove metal ions from wastewater across 5 cycles without affecting the original abosotption capacity, showing their applicability for continuous process design (Nassar, 2010). Apart from that, Fe_3O_4 nanosorbents also play a role as efficient and affordable adsorbents for the quick separation and recovery of other metal ions from wastewater effluents. Since heavy metals are hazardous to humans, animals, and plants as well as have a tendency to bioaccumulate even at low concentrations, so, the ability to synthesize MNPs with the capacity to adsorb heavy metals is leading to the huge advancement in the environmental remediation technology.

Other than that, magnetophoresis also can be employed in the removal of microalgae from polluted water sources such as ponds and river. The recent research verified the potential for using surface-functionalized IONPs to remove microalgae out of fishpond water. Based on the concentration of surface functionalized iron oxide nanoparticles (IONPs) utilized, microalgae removal efficiencies of over 90% are achievable. The used IONPs have a saturation magnetization of 113.8 emu/g and have been surface functionalized with a cationic polyelectrolyte to facilitate their electrostatic adhesion to microalgae cells (Toh et al., 2012).

As IONPs have huge surface area, they can offer huge amount of functional groups for the absorption of organic pollutants, which leads to their excellent capacity for the adsorption process. Typically, organic pollutants were adsorbed through surface exchange processes, much like with heavy metals, until all the surface functional sites were saturated. After then, pollutants may be able to penetrate deep into the adsorbent, where they can have further interactions with the functional groups (Xu et al., 2012). For example, MNPs are surface-modified with carboxymethyl cellulose (CMC) to form cellulose-coated $Fe_3O_4@SiO_2$ coreshell magnetic nanoparticles in the removal of ethylene blue carboxymethyl (Zirak et al., 2017). Indeed, on the surfaces of MNPs functionalized with appropriate materials, the dye catalytic degradation and adsorption may proceed simultaneously. It is also worth noting that MNP may be used repeatedly since magnetic nanocomposites for dye adsorption are very reusable.

2.1.2(b)   Biomedical Applications

Apart from that, MNPs are popularly employed in a variety of biological applications due to their wide range of physicochemical characteristics, simplicity in synthesis, stability, and biocompatibility. In addition, MNPs' remote motion control through an external magnetic field makes them helpful in a wide variety of biological applications. Drug delivery, hyperthermia, biomolecule extraction, and optical imaging are just some of the many applications that have found success using MNPs.

Drug delivery is one of the vital therapeutic applications of MNPs. The transfer of pharmaceuticals and bioactive substances (peptides, proteins, DNA, etc.) over the cell membrane and into cells is known as drug delivery or cellular delivery, and it is an essential procedure in the biomedicine industry. Unfortunately, direct drug and biomolecule delivery is typically ineffective and suffers the issues of degradation. Thus, the use of an appropriate targeted drug delivery system can improve the efficacy of an active substance by transporting drugs to targeted locations without causing the side effects caused by high drug concentrations in other cells or organs. In this regard, MNPs are the most promising choice as the drug carrier in the human body because of

their inherent magnetic nature, which allows them to be remotely controlled by an external magnetic field in a noncontact mode. During the drug delivery process by using MNPs, the magnetic force imposed on the drug loaded MNPs must be carefully controlled so that it can overcome the opposing viscous force that hinders their motion in the blood or biological fluid (with relatively high viscosity). Therefore, magnetophoretic mobility of MNPs in the blood or biological fluid, (which is a measurement of a magnetic carrier's mobility in a fluid solution under the effect of magnetic field), is one of the critical factors that need to be considered and improved in the application of MNPs in drug delivery (Tartaj et al., 2016).

In addition, MNPs are important in the hyperthermia treatment. It is known that heating organs or tissues to temperatures between 41 and 46 °C can destroy cancer cells, making hyperthermia a promising biological therapy. Regarding biological reaction and application method, both therapies behave radically differently. The damage that classical hyperthermia causes to cells and tissues is pretty much completely reversible, but it increases the radiation harm to tumor cells and the effectiveness of chemotherapy. The core purpose of current therapeutic hyperthermia studies is to maximize thermal uniformity in the treatment area at moderate temperatures (42-43°C). Nonetheless, it needs substantial technical work as well as sophisticated treatment and thermometry equipment (Hilger, Hergt and Kaiser, 2005). Cancer cells are more vulnerable to hyperthermia than healthy cells because they exist in an environment with a lower pH and poorer thermotolerance. Hyperthermia is seen to be an useful treatment of cancer since it generates localized hysteric heat that is focused and causes less heating of surrounding tissues. In addition, the ability of MNPs-based hyperthermia treatment to penetrate into deep tissues and destroy cancer cells specifically while avoiding healthy tissues from damage is the key benefit (Ali et al., 2021).

2.1.3   Advantages and Disadvantages of MNPs

MNPs demonstrate high potential to be employed in various engineering as mentioned above because of some special advantages that they possessed as compared to their bulk counterpart or other materials. In this subsection, some general advantages of MNPs are summarized. In addition, it is also the purpose of this section to briefly explain the disadvantages of MNPs and relate the biocompatibility of MNPs to their size. Firstly, MNPs can display the superparamagnetic characteristic that is favorable for many engineering applications. For instance, for a MNP with size smaller than superparamagnetic limit of its material (such as 35 nm for magnetite Fe_3O_4), the MNP will behave as a superparamagnetic particle with extraordinarily high magnetization under the presence of magnetic field (as similar to ferromagnetic materials) but zero coercivity (the magnetization vanishes upon the removal of the magnetic field, as shown by paramagnetic materials). The unique ability to manipulate the particles' colloidal behaviour and mobility is made possible by their superparamagnetic behaviour, which allows one to switch the magnetization on and off by applying external magnetic fields. This feature is particularly useful in the environmental treatment and medicinal industries, when the ability to remotely control the mobility of MNPs is quite desirable.

Secondly, MNPs has extremely huge surface-area-to-volume ratio due to their tiny size, which can provide abundant surface area for adsorption and reaction activities by using only trivial amount of material. However, the full dispersion of MNPs in the fluid suspension can be thermodynamically non-favorable, due to exceptionally high surface energy displayed by the MNP system under such configuration, and they have the high tendency to form aggregates that reduces the overall exposed surface area. Under this scenario, the MNP system is denoted as colloidally unstable. Presently, there exists a scientific progression in the production of colloidally stable MNPs that offer a substantial specific surface area for adsorption and reaction processes. This is achieved through the functionalization of the MNPs' surface with polyelectrolytes, which impose electrostatic repulsion and steric hindrance to prevent the formation of aggregates. For instance, the anti-cancer medicine doxorubicin and the polyethylene glycol (PEG) molecule can be attached to the surface of magnetic iron oxide nanoparticles to kill tumour cells selectively.

Because of the PEG molecule's facilitation of intracellular transport while the doxorubicin is able to kill off the selected tumour cells (Gambhir et al., 2022).

The utilisation of MNPs in the biomedical field presents certain challenges pertaining to their biocompatibility and potential toxicity to the human organism. It has been revealed that several parameters, including size, surface area, surface modification, and aggregation state would affect how hazardous nanomaterials are. Particles with a size greater than 10 nanometers are recommended to evade renal filtration and facilitate rapid penetration. However, it is crucial that the particle size remains below 200 nanometers to prevent retention from the circulation, in which they concentrate and are discharged through the hepatic filtration and mononuclear phagocyte system. The uses of MNPs in different applications in biomedical fields strongly depends on the size of MNPs used. In drug delivery application, MNPs with high specific surface area are surface coated with high density of receptors, which are employed to boost local drug concentration and regulate drug release. Consequently, as surface area increases, more chemical reactions take place and the toxicity of MNPs becomes less under control (Li, Li, Wang and Liao, 2021). In addition, the size, shape, and biodistribution of the carrier particles have a significant impact on the particles' ability to target the circulatory system at the vascular level (Shaw, Shit and Tripathi, 2022). Therefore, it is essential to obtain an MNP system with a narrow size distribution and uniform geometry, especially for applications related to the biomedical field.

2.2   Magnetophoresis of MNPs

The movement of MNPs in relation to their surrounding fluid when a gradient of magnetic field is applied externally is known as magnetophoresis. Classical magnetophoresis theory assumes that all particles in the dispersion are moving individually upon exposure to an external magnetic field, and their motion is manipulated by a few forces acting on them.

Initially, the magnetic force, denoted as F_{mag}, is exerted on the magnetic nanoparticles (MNPs) as a result of the magnetic dipole moment response within the MNPs to the external magnetic field, which can be mathematically written as:

$$F_{mag} = \mu \nabla B \tag{1}$$

where μ indicates the magnetic dipole moment of MNPs, B is the magnetic flux density and ∇B is the magnetic field gradient. Here, the magnetic dipole moment possessed by each MNP can be computed by its magnetization which is defined as the density of dipole moment (on volume basis):

$$M = \frac{\mu}{V} \tag{2}$$

where M is the magnetization and V is the volume of the MNPs. By combining equation (1) and (2), the magnetic force, F_{mag} acting on a spherical MNPs can be expressed as:

$$F_{mag} = VM\nabla B = \frac{\pi d^3}{6} M\nabla B \tag{3}$$

where d is the diameter of the MNP.

In addition, MNPs also experience viscous force, F_d during magnetophoresis, which is the resistance to the motion of MNPs imposed by the surrounding fluid. According to Stoke's law, the viscous drag force experienced by a spherical MNP is given by:

$$F_d = 3\pi\eta d_H v \tag{4}$$

where η is the viscosity of the suspension, d_H is the hydrodynamic diameter of MNPs and v is the magnetophoretic velocity of the MNP (in relative to the fluid).

As magnetophoresis of MNP is conducted on the Earth under the gravitational field, each MNP also can experience gravitational force (that is exerting a pulling force downwards) and buoyant force (the action of which is upward), which can be formulated as:

$$F_g = mg \tag{5}$$

where m is the mass of the MNP,s and g is the gravitational acceleration (with the value of 9.81 ms-1 near the Earth surface),

The buoyant force is given by:

$$F_b = \rho_f g v \tag{6}$$

where ρ_f is the density of fluid and v is the magnetophoretic velocity of MNPs.

However, due to the size of MNPs being extremely small, the gravitational force and buoyant force can often be neglected as compared to other forces acting on MNPs during magnetophoresis.

Last but not least, there is also a Brownian force acting on all MNPs subjected to magnetophoresis. Brownian force is a random force acting on the MNP originated from the random bombardment of the surrounding fluid particles on the MNPs, from a macroscopic perspective, this results in MNPs diffusing along the MNPs concentration gradient. Due to the random nature of the Brownian force, it cannot be expressed explicitly like the aforementioned forces, however, the significance of the Brownian force can be reflected by the magnitude of diffusivity, which can be formulated by Stokes-Einstein equation as shown below

$$D = \frac{k_B T}{6\pi\eta R_h} \tag{7}$$

where kB is Boltzmann constant, T is absolute temperature, Z is the dynamic viscosity of fluid and Rh is the hydrodynamic radius of the MNPs

According to Newton's second law of motion, the acceleration of MNPs is depending to the net force acting on it (Brownian force is not considered in this analysis):

$$\sum F = m\frac{dv}{dt} = F_{mag} + F_d$$

However, in the magnetophoresis of MNPs, the inertial term ($\sum F$) is negligible due to the low Reynold number environment. Thus, the inertial term is considered to be zero while describing the dynamics of the MNPs during magnetophoresis:

$$0 = \frac{\pi d^3}{6} M \nabla B + 3\pi \eta d_H v \qquad (8)$$

Therefore, the magnetophoretic velocity can be determined from the equations (8) as:

$$v = -\frac{\pi d^3 M \nabla B}{3\pi \eta d_H} \qquad (9)$$

The concentration profile of the magnetophoretically exposed MNP solution may be determined by solving the drift-diffusion equation using the formula for magnetophoretic velocity presented below:

$$\frac{\partial c}{\partial t} = D\nabla^2 c - \nabla \times (vc) \qquad (10)$$

where c is concentration of theMNPs solution, v is magnetophoretic velocity of MNPs and D is diffusivity of MNPs in the solution, which can be calculated using Einstein–Stokes equation as mentioned above.

Classical magnetophoresis theory has been used to predict the dynamical behaviour of the magnetophoresis process, however it has certain drawbacks. At first, the dipole-dipole interactions between MNPs are neglected in this model, thus, the MNP concentration and magnetization has to be sufficiently small so there is no significant aggregation of MNPs in the magnetophoresis process to be studied (Leong et al., 2017). Secondly, this model assumed only one-way momentum transfer from the surrounding fluid to the MNPs (due to the viscous force imposed on the MNPs), however, the momentum transfer at the opposite direction (from MNPs to fluid) has been neglected. Therefore, the use of this model requires the concentration of MNPs to be low so that the net reactive force of MNPs on the fluid can be negligible. Thus, it is important to investigate the MNP/MNP interaction and MNP/fluid interaction more thoroughly and incorporate these effects into the classical magnetophoresis theory, so that the predictability of the model on the magnetophoresis process can be further enhanced.

2.2.1 Cooperative Effects

Researchers have found that the magnetophoretic velocity they detect in the lab exceeds what can be predicted with only traditional magnetophoresis theory (De Las Cuevas et al., 2008). The deviation of the prediction from the experimental results indicates that there are some dominating mechanisms that are missing in the classical magnetophoresis theory. One of them is the cooperative effect, which originated from particle aggregation.

The aggregation of MNPs is resulted from the interaction between magnetic dipole moments possessed by each MNP.it has been verified from the experiment that When subjected to a magnetic field, MNPs will self-assemble into structures that are extended and linear in shape (Leong et al., 2020), which will further interact over time and generate lengthier and larger aggregates. These aggregates are reversible due to the superparamagnetic property of the MNPs. When the external magnetic field is removed, the MNPs lose their magnetization and magnetic attraction which subsequently regenerate the original suspension. The interaction between two magnetic dipole moment with a separation distance of *r* can be formulated as follows (Faraudo and Camacho, 2009):

$$U_{dd} = \frac{\mu_o \mu^2}{4\pi r^3}(1 - 3cos^2\theta) \tag{11}$$

where $\mu_o = 4\pi 10^{-7} NA^{-2}$ is the magnetic permeability of free space and θ is the angle between the direction of the external magnetic field and the line joining the centers of the two particles. See **Figure 2.2** for a visual representation of the geometry of the interaction between two colloidal particles, each having a dipolar moment of m in the direction of an applied magnetic field.
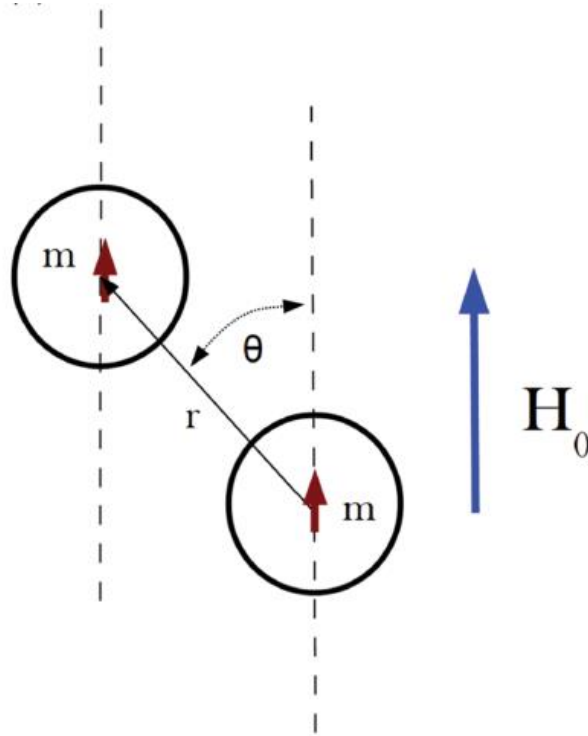
Figure 2.2: A schematic showing the geometry of the forces exerted by a magnetic field on two colloidal particles, each with a dipolar moment of m (Faraudo, Andreu, Calero and Camacho, 2016).

In addition, another parameter was introduced to characterize the strength of cooperative effect of (or MNP aggregation), namely magnetic coupling parameter, Γ which is defined as:

$$\Gamma = \frac{|U_{dd}^{max}|}{k_B T} = \frac{\mu_o m_s^2}{2\pi d^3 k_B T} \qquad (12)$$

where $k_B T$ is the thermal energy ($k_B = 1.38 \times 10^{-23} \, JK^{-1}$ is the Boltzmann constant and T is the temperature). This measure provides the ratio of the energies of magnetic interaction and thermal fluctuations between two contacting MNPs. In addition, it should be noted that the particles are considered at saturation magnetization with total magnetic dipoles moment of m_s in equation (10), which implies both energies are compared under the scenario that the MNP possess the largest possible magnetic dipole moment under an intense magnetic field. Thus, the parameter Γ contrasts the thermal energy with the strongest possible level of the attractive particle-particle magnetic

interaction. Physically, the scenario with, Γ bigger indicates that magnetic interactions are present in the MNP system, whereas thermal agitation is dominant and the magnetic attraction between the MNPs is absent for the opposite case (Faraudo, Andreu and Camacho, 2013).

Moreover, another crucial parameter to measure the significance of cooperative effect in magnetophoresis is the aggregation parameter, N^*. This dimensionless aggregation parameter N* are derived based on thermodynamic approach, whichrelate the degree of particle interaction to the magnetic characteristics of the MNPs as well as thermodynamic values like concentration and temperature. In this context, N* = 1 is the critical value for field-induced aggregation of MNPsParticles will form lengthy structures (simple chains for N* 10 and bundles of chains for larger values of N*) if N* is greater than 1. On the other hand, if N* is less to 1, the creation of aggregate is not feasible and the entropy of the system will prevails. The magnitude of N^* for a particular MNP system can be calculated as follows:

$$N^* = \sqrt{\phi_0 e^{(\Gamma-1)}} \qquad (13)$$

where ϕ_0 is the volume fraction of MNPs in the solution.

According to the magnitude of both and N^*, the interaction nature of MNPs can be categorized into a few regimes. Naturally, if thermal energy is greater than the magnetic interaction, $\Gamma < 1$ and thus $N^* < 1$. As the result, there is no chain formation or occurrence of particle aggregation. However, when $\Gamma > 1$, this means that the magnetic interaction energy is more than the heat energy, but it doesn't prove that chains will form. This is because N^* is also depending to volume fraction (or concentration) of MNPs. Therefore, if $\Gamma > 1$ and $N^* > 1$, aggregation of MNPs would happen and can be significant (Leong et al., 2020). If field-induced aggregation is undesirable, then the process must operate in circumstances of Γ less than 4, else the concentration of the dispersion needs to be carefully managed to be low enough to ensure that N* is still less than 1. In contrast, for particles with $\Gamma > 15$, aggregation of particles ($N^* > 1$) will always be inevitable, even under very diluted settings.

Individual particles typically move at relatively low speeds during magnetophoresis due to the large viscous drag experienced by the tiny particles moving in a viscous environment. A large aggregation parameter ($N^* > 1$) can significantly accelerate the magnetophoresis process as observed magnetophoretic velocities of MNP aggregated exceed their corresponding single particle by orders of magnitude. So, these MNPs collide to form bigger aggregates that move much faster (Faraudo, Andreu and Camacho, 2013).

2.2.2   Hydrodynamics Effect

Magnetophoretic force experienced by MNPs in various places will be different according to the traditional view of magnetophoresis when there is existence of an inhomogeneous magnetic field gradient within the system. As shown in **Figure 2.3,** the lower region of the system which is near to the magnet has the greater magnetic field strength as compared to the upper region. Thus, after the initiation of magnetophoresis, the concentration of MNPs at the lower region would be lesser as compared to the upper region due to the rapid MNP collection at the lower region, according to the prediction by using classical magnetophoresis theory. This theoretical prediction, however, runs counter to what was observed experimentally during a magnetophoresis experiment, when it was found that the concentration of MNPs in the system stayed constant during the whole procedure, with the total concentration falling with time (Leong et al., 2020). This uniform distribution of MNPs throughout the whole solution during magnetophoresis suggests the presence of a driving force responsible for this distribution. Magnetophoresis-induced convection is the primary source of this driving force. Since the ambient fluid is not magnetically sensitive, it requires momentum from the motion of the MNPs to start convection during magnetophoresis. Moreover, hydrodynamic effect of magnetophoresis refers to the interaction between MNPs and fluid that is necessary for momentum from moving MNPs to be conveyed to the ambient fluid and cause convection.
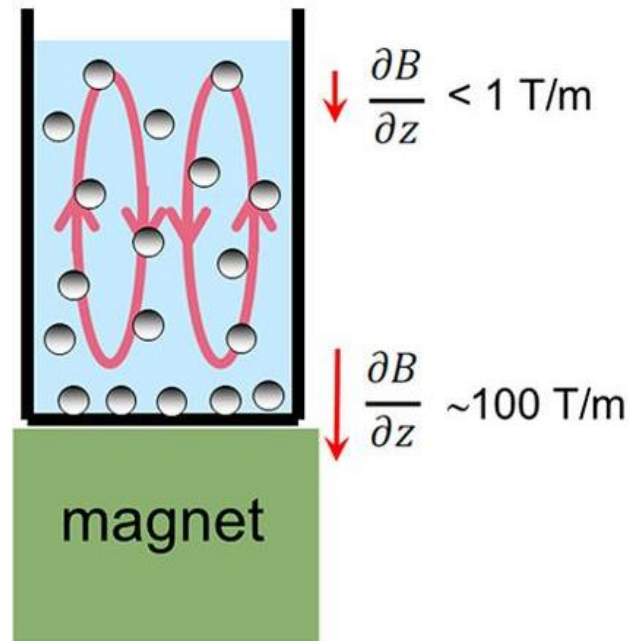
Figure 2.3: A simple setup uses a single permanent magnet to observe magnetophoresis caused by convection (Leong et al., 2020).

A dye-tracing experiment provides more evidence that magnetophoresis-induced convection is present (as shown in **Figure 2.4**), in which a concentrated dye is injected into the MNP solution to track the fluid motion in it during magnetophoresis. It can be observed that the dye rose rather quickly and homogenized throughout the entire fluid rapidly upon subjected to magnetophoresis. The fluid convection indicates that the fluid possess momentum, which is transferred from the moving MNPs into it. Thus, the two ways momentum transfer (from fluid to MNPs and from MNPs to fluid) can be remarkable and play a crucial role in governing the dynamical behavior of MNP solution during magnetophoresis. It is undeniable that the homogenization of the suspension and the enhancement of MNP dispersion within the solution are the results of the mixing process generated by this convective flow (Leong, Ahmad and Lim, 2015) throughout the entire magnetophoresis.
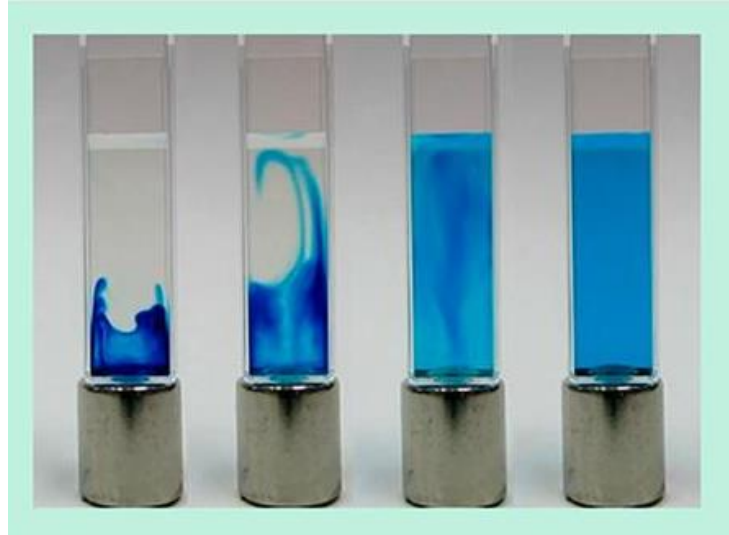
Figure 2.4: Magnetophoresis visualization of convective flow using a blue dye (Leong et al., 2020).

However, the low regional resolution of the magnetic field is one of the method's major shortcomings, is now proven to have a significant potential to be overcome by the hydrodynamic effect. Magnetic separation of MNPs originally positioned in the region far from the magnet is unsuccessful because the magnetic field is extremely weak as one advances away from the magnetic source. However, induced convection has a longer-range influence, in which the convective flow at the far end region is still proven to be strong enough to attract MNPs toward the magnetic source (in comparison to individual magnetophoretic velocity) (Leong et al., 2020).

In order to describe the importance of hydrodynamic effect (or magnetophoresis induced convection), magnetic Grashof number Gr_m, which can be mathematically expressed as:

$$Gr_m = \frac{\nabla B \left(\frac{\partial M}{\partial c}\right)_H (c_s - c_\infty) L_c^3}{\rho v^2} \tag{14}$$

where ρ is the mass density of MNPs solution, c_s is the MNPs concentration at the collection plane (surface adjacent to the magnet), c_∞ is the bulk concentration of MNPs, L_c is the characteristic length of the system subjected to magnetophoresis and v is the kinematic viscosity of the solution (Leong, Ahmad and Lim, 2015). Magnetophoresis is compared to natural convection in a fluid with a heated plate below

to derive Equation (12). The ratio of the magnetic buoyant force to the viscous force is the definition of the magnetic Grashof number. Magnetic buoyancy effect and magnetophoresis-induced convective flow are thus important features of an MNP system exposed to magnetophoresis if the magnetic Grashof number Gr_m is more than unity (Leong et al., 2020). On the other hand, magnetophoresis induced convection is not significant for the case with Gr_m less than 1, which implies that the magnetophoresis kinetics is well described by the classical magnetophoresis theory. In fact, it has been predicted that the magnitude of Gr_m of a MNP solution is still more than one even at the extremely low MNP content (as compared to the range of concentration of MNP solution used in industrial applications). Thus, the dynamical behaviors of the magnetophoresis process in various applications are heavily influenced by the magnetophoresis induced convection. For instance, according to the calculation performed by Leong, Ahmad and Lim (2015), the Gr_m is less than unity only when the concentration of MNP is lower than 0.05 mgL^{-1}, which is a very low concentration to be employed the industry. That being the case, hydrodynamic effect is the critical factor that governs the kinetics of most magnetophoresis processes, especially for those conducted under a batchwise mode (Leong, Ahmad and Lim, 2015).

2.2.3   HGMS vs LGMS

Magnetic separation (MS) process of MNPs from their solution involves the utilization of an external magnetic field gradient to generate magnetophoretic force on the MNPs and collect them in a specific region. Magnetic separation can be classified as either low-gradient (LGMS) or high-gradient (HGMS) depending on the strength of the magnetic field gradient used. Both of these MS schemes have shown successful results in solving biomedical, engineering as well as environment problems. Despite of that, HGMS is widely used in the past decades and has been well-established as compared to LGMS. However, development and applications of LGMS are spiking in the current years due to various advantages offered by these MS schemes.

HGMS is widely used in variety of areas such as kaolin clay benefaction and removal of environmental contaminants, heavy metal ions, dyes as well as non-metal contaminants. The central component of the HGMS system is an electromagnet housing a packed bed column of magnetically susceptible wires with a diameter of around 50µm. When a magnetic field is applied across the column, the wires dehomogenize the field and generate strong field gradients around the wires, which attract and keep MNPs affixed to the wires' surfaces (Moeser et al., 2004). The illustration of HGMS operation is show in **Figure 2.5(a).** The main highlight of HGMS is the localized high magnetic field (> 100 T/m) is generated near to the wires when electromagnet is switched on. For instance, it has been demonstrated that a magnetic field gradient of up to 1260 T/m may be produced in close proximity to the wires inside the HGMS column. According to equation (3), the strength of the magnetophoretic force is related to the incline of the magnetic field. Thus, the MNPs will experience enormous magnetophoretic force as it flows through the area in the vicinity of the wires, which enable them to overcome other opposing force such as viscous drag and Brownian forces and gives rise to effective magnetic separation (Leong, Yeap and Lim, 2016).

On the other hand, as compared to complex set up in the HGMS column (with the insertion of magnetizable wires), the design of LGMS separator is relatively simpler. This is because LGMS system involves only the magnetophoresis of MNP solution by using hand-held permanent magnet(s) without requiring any packing to be installed in the column. Since the magnetic field gradient decreases rapidly with distance from the magnet, the magnetic field gradient generated across the MNP solution is typically less than 100 T/m in the LGMS system (Yavuz et al., 2006). **Figure 2.5(b)** demonstrates the setup of LGMS which only includes a permanent magnet and a container filling with the MNPs solution. The magnetophoresis process begins as soon as the magnet is put either at the side or at the bottom of the separator, which triggers the MNPs to move towards the magnetic source and causes them to be isolated from the solution (Leong, Yeap and Lim, 2016). Despite of the low magnetic field gradient, LGMS has been proven to be feasible in environmental treatment and medicinal industries if the cooperative and hydrodynamic effects of magnetophoresis are exploited to improve the separation rate of MNPs induced by the LGMS system.
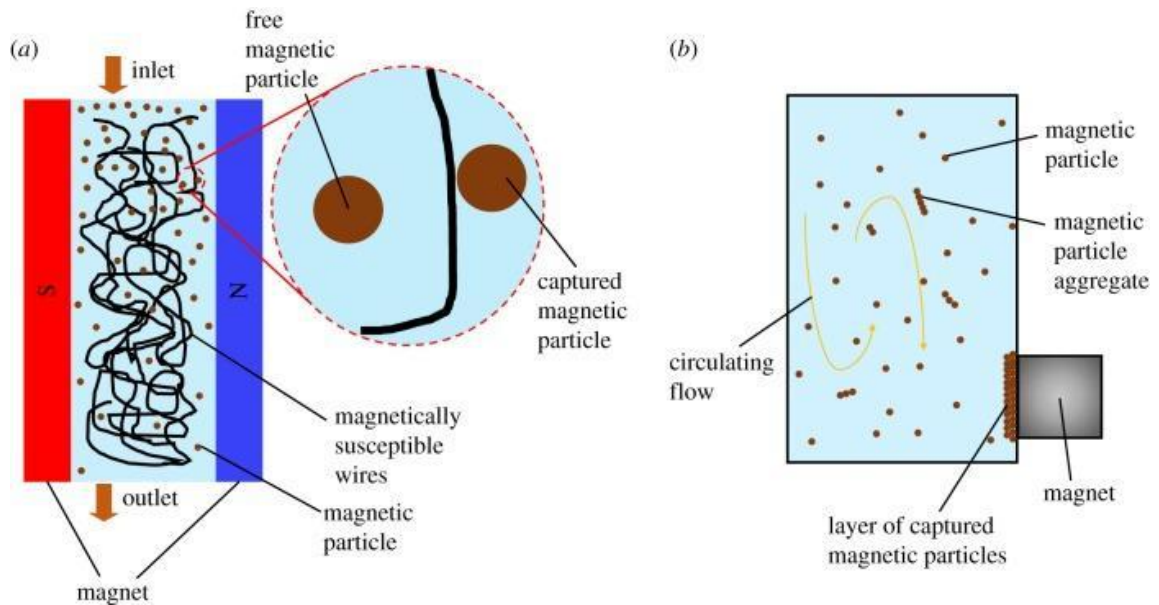
Figure 2.5: Demonstration of HGMS (a) and LGMS (b) processes (Leong, Yeap and Lim, 2016).

Despite the fact that HGMS is well developed and frequently used in a variety of applications, the use of magnetizable wires to generate a strong magnetic field gradient is problematic in several ways. Since the electromagnet needs a lot of power to generate a magnetic field strong enough to induce rapid separation of MNPs, the HGMS is not cheap to set up and maintain (Toh et al., 2012). Due to the highly randomised inhomogeneous magnetic field produced by the randomly entwined magnetizable wire, it is challenging to construct an analytical model to implicitly explain the HGMS process quantitatively (Moeser et al., 2004). Also, MNPs can permanently adhere to and accumulate on the wires after the separation operation and they are challenging to be removed, which causes the reduction of the separation effectiveness of HGMS column in the subsequent operation cycles (Gómez-Pastora, Bringas and Ortiz, 2014).

On the contrary, LGMS has addressed the drawbacks of HGMS that are mentioned in the previous paragraph. The electromagnet in an HGMS consumes a lot of power, whereas the permanent magnet(s) in an LGMS can be operated with little more than the human hand. Besides that, the design of LGMS is very simple as compared to HGMS column with magnetizable wires packed inside it, which

significantly simplifies its maintenance process and reduce the maintenance cost. However, a major drawback of LGMS is that the low magnetic field gradient throughout the MNP solution results in a relatively weak magnetophoretic force for the MNPs to experience. But, the separation efficiency of LGMS can be improved by exploiting cooperative and hydrodynamic effects in its design. Evidently, by the aid of cooperative effect, the MNPs are moving as a larger aggregates or clusters with greater magnetophoretic force, which can be separated approximately 69 times faster as compared to the case without the consideration of cooperative effect (De Las Cuevas, Faraudo and Camacho, 2008). In addition, the hydrodynamic effect also has been proven to improve the separation rate of MNPs induced by a LGMS system by 27 times (Leong et al., 2015).

2.2.4   Batch and Continuous flow mode of magnetophoresis.

In many studies related to LGMS, the separation process is conducted in a batchwise manner. Here, the separation of MNPs is conducted in a batch container and the solution is removed manually after the removal of MNPs from their suspension. At first, the MNPs is mixed with liquid solution in the aid of agitation. Then, the MNPs mixture solution is transferred to a separator with magnet(s) put at the side to induce the occurrence of magnetophoresis. At the end, the clear solution will be drain out from the separator and the MNPs will be recollected. Such a batchwise separation of MNPs from the solution was usually conducted in small scale, thus, batch or semi-batch operation mode of LGMS typically requires a high level of manual adjustment or supervision and labour demand (see **Figure 2.6 (a)**). Therefore, the LGMS in batchwise mode is not ideal to be directly applied at an industrial scale. In this regard, the attractiveness of incorporating the 'continuous flow' element of HGMS into the LGMS system is that it makes the LGMS process amenable to automation, facilitation, and industrial-scale operation. Continuous flow low gradient magnetic separation (CF-LGMS) is the consequence of incorporating 'continuous flow' into the LGMS system, as shown in **Figure 2.6 (b)**. The main difference between batchwise and CF-LGMS is the presence of pump in the CF-LGMS system which continuous pump the MNP solution into the separator column where separation process is taking place. A CF-

LGMS process is typically operating in this manner: After the MNP mixture solution formed by the agitation tank, it will be transferred to the separator through a pump. The solution flows continuously through the magnetic separator where there is the occurrence of magnetophoresis. The clear solution will be released from another end of the separator and MNPs will be retained in the separator the magnet(s).
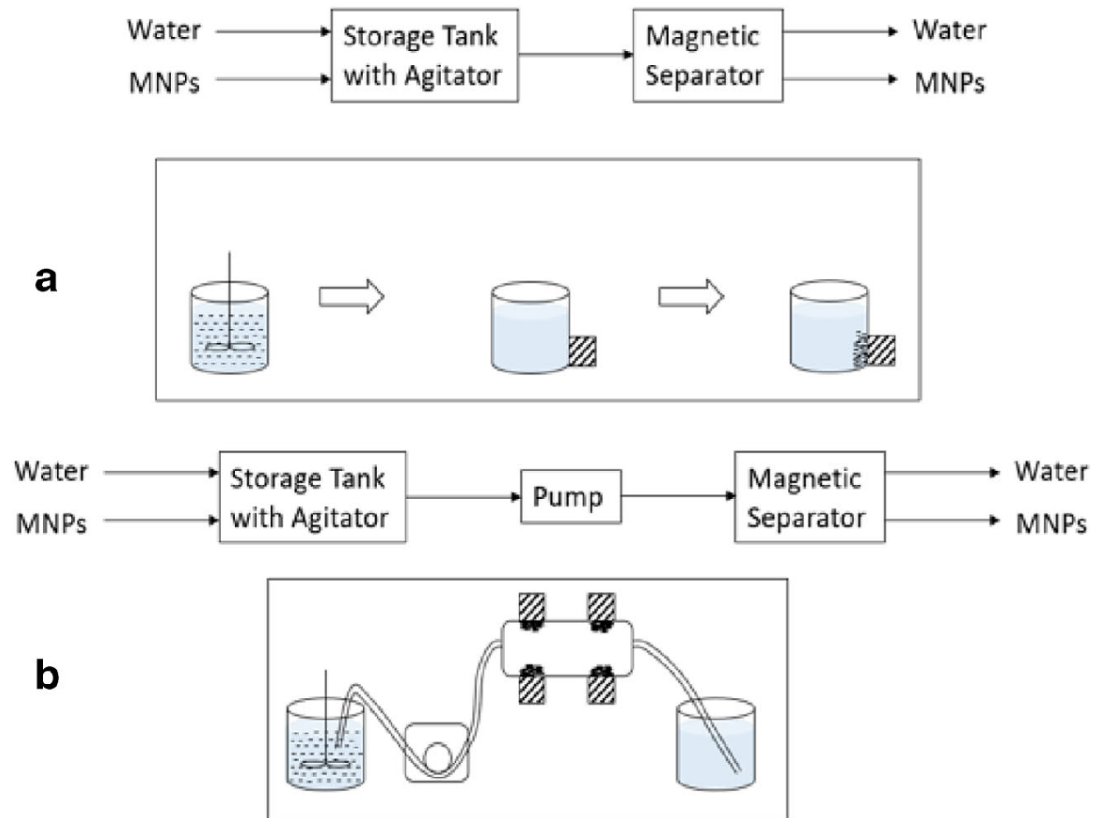
Figure 2.6: Demonstration of LGMS in batchwise (a) and continuous flow mode (b) (Chong et al., 2021).

After comparing the operating process of batchwise and CF-LGMS, it is crystal clear that CF-LGMS is better than batchwise in term of automation. If the LGMS process is to be scaled up in a batchwise fashion, a separation vessel of huge capacity is needed. As the batchwise operation procedure is manually regulated, as the consequence, the labor cost for its operation can be significantly expensive. Another drawback of batchwise magnetic separation originates from the difficulties of remote operation and automation, which runs against to mainstream industry developments that promote the integration of automatic systems into the manufacturing line. So, batchwise LGMS technique is neither practical nor appropriate for use in real-time

industrial applications which running at extremely large scales. All these disadvantages of batchwise LGMS can be overcome by employing CF-LGMS in variety applications. (Chong et al., 2021).

2.3   Degree of Monodispersity MNPs

In comparison to their bulk particles, MNPs have particularly special physical and chemical characteristics. The unique properties of MNPs, particularly their magnetic and magnetophoretic properties, adsorption capacity, catalytic performance, biocompatibility and etc., are strongly influenced by their size. For example, according to equation (3), the magnetophoretic force experienced by MNPs is depending on the size, in which a larger MNP will experience strong magnetic force and being separated more rapidly. In addition, the superparamagnetic property can only be observed for MNPs with size smaller than the superparamagnetic limit, and the MNPs that are larger than this limit might display some sort of ferromagnetism. Therefore, the well control and manipulation of MNP size during the synthesis is essential to tailor a MNP system that is appropriate for a particular application. Besides that, due to the cooperative effect that takes place during magnetophoresis, MNPs aggregates will formed during the magnetophoresiswith various size will be formed, which subsequently increase the polydispersity of the MNP system and alter . Because of this reason, their magnetophoretic properties of the clusters also will be changed. Therefore, selecting selection of the MNPs with proper particle size which fulfills the needs of the intended application and ability to maintain its size distribution during the operation is crucial because these size-dependent properties are one of the most significant elements in deciding theto ensure the feasibility of practically MNPs and safety of the applications all engineering applications that include the usage of MNPs (Yeap et al., 2014). In this regard, the ability to synthesis and produce a monodisperse MNP system with uniform size is important to facilitate the usage of MNPs and ensure the safety in various technological processes.

　　　　To quantify the monodispersity of a particle system, there are several parameters that are oftenly used. Standard deviation, σ is one of the parameters to

characterize the size distribution or the dispersity of particle system quantitatively, which is given by:

$$\sigma = \sqrt{\left(\frac{\sum(d-\underline{d})^2}{n-1}\right)} \qquad (15)$$

where d is the diameter of the MNPs, $\underline{d}$ is the mean diameter of MNPs and n is the number of population. Based on equation (15), standard deviation is a measurement that describes how far away the size of each MNPs deviated from the mean value (Wechsler, 1997). It measures how far the data are scattered from the mean. When the standard deviation is low, the majority of the particle sizes are grouped around the mean; conversely, when the standard deviation is large, the particle sizes are more spread. The majority of the particle sizes are likely close to the mean, and the particle system is likely to be very monodisperse, according to the standard deviation that is close to zero. Based on the size distribution curves as shown in **Figure 2.7**, the curve at the bottom is more concentrated around the mean, which causes it to have the smaller standard deviation as compared to the size distribution located at the top (the particle size is more widely spaced out).
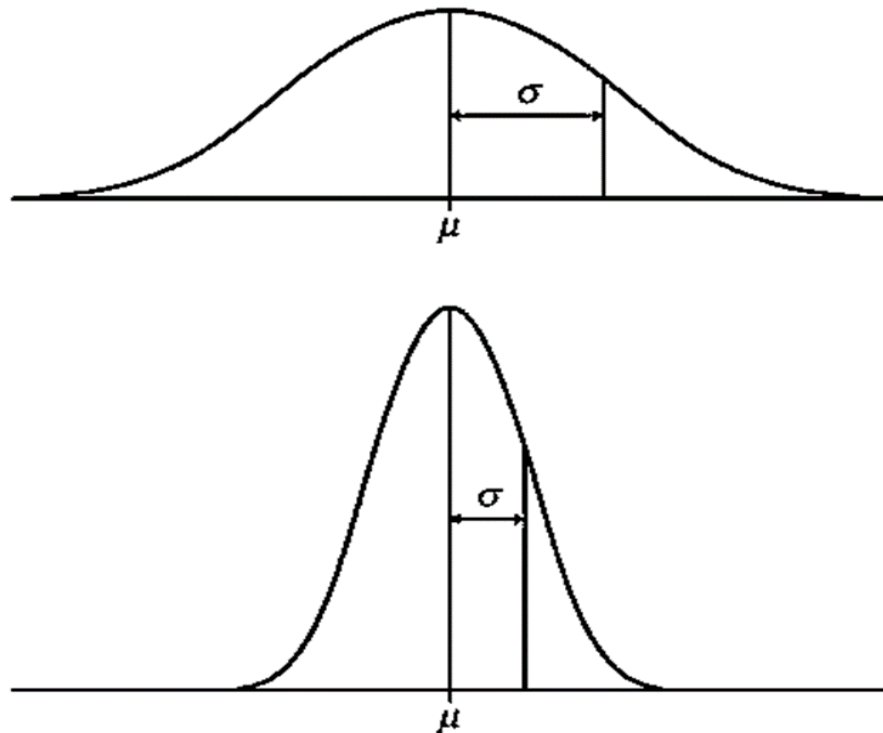
Figure 2.7: High and low standard deviation curves (Standard Deviation, 2022).

The polydispersity index (PDI), a different parameter, quantifies a particle system's dispersity. The polydispersity index is mathematically expressed as:

$$PDI = \left(\frac{\sigma}{\underline{d}}\right)^2 \qquad (16)$$

According to equation (16), the PDI is calculated by dividing the square of the standard deviation by the mean particle diameter. (Raval et al., 2019). In reality, the PDI value can range from 0 to 1, with values more than 0.3 indicating polydisperse particle size distributions and values less than 0.3 implying monodisperse particle system. Therefore, PDI is used to determine the average homogeneity of a particle solution, and higher PDI values denote a wider size dispersion in the particle sample. Additionally, PDI may show the homogeneity and efficacy of surface functionalization throughout the whole particle sample as well as nanoparticle aggregation (Clayton, Salameh, Wereley and Kinzer-Ursem, 2016).

Furthermore, confidence level is also a parameter to describe monodispersity of a particle system. In statisticsWhile describing the monodispersity of a particle system, a confidence interval reflects the likelihood that the size of a particle a population parameter would lie between a range of values for a given fraction of the timearound its mean. Which meansIn other word, confidence intervals quantify quantifies how definite or uncertain a sampling techniquethe size of a particle in the system is. It The value of confidence level to describe the monodispersity of a particle system can be selected from various probability limits, with a 95% or 99% confidence level being the most preferred (Hayes, 2022). With a specific value of confidence level, a MNP system has the greater degree of monodispersity if the confidence interval has the smaller range.

Nowadays, numerous synthesis methods proposed by many researchers are able to produce highly stable, narrow size distribution and well-controlled shape or morphology (Faraji, Yamini and Rezaee, 2010). As described in **Section 2.1.1**, the popular chemical methods are co-precipitation, thermal decomposition, hydrothermal and microemulsion, in which the monodispersity, pros and cons of each synthesis method has been tabulated in **Table 2.2**. Among these techniques, the most beneficial way for creating MNPs is likely to be the hydrothermal process. Due to its benefits in

creating NPs with appropriate size, shape, high crystallinity, and uniform composition, the hydrothermal technique is flexible and outperforms alternative methods. In addition, the benefit of hydrothermal method to generate well-controlled and narrow size distribution NPs is due the reduce in probability of agglomeration (Zahid et al., 2019). On the other hand, in terms of monodispersity (PDI value), the thermal deposition and the hydrothermal synthesis method have the lower value as compared with the other method. This indicates that the standard deviation of the size distribution is narrow and centralized to the average particle size. Conversely, other two techniques (co-precipitation and microemulsion), have higher PDI values. That means, the size distribution curves will be wider as compared to the other two techniques. As the preferable method is the hydrothermal synthesis method, the cons of it is high temperature and pressure are required. However, it can create monodispersed nanoparticles with diverse morphologies.

Table 2.2: Monodispersity of MNPs produced by various method

Synthesis Method	Size distribution (nm)	Monodispersity (PDI)	Pros	Cons	References
Co-precipitation	8.5 ± 1.5	0.0311	Simple process, quick and easy technique of preparation, and simple control of particle size and composition	Significant aggregation, poor morphology, and unequal distribution of particle sizes	(Kang, Risbud, Rabolt and Stroeve, 1996)
Thermal decomposition	12 ± 1.4	0.0136	Generating particles with a narrow size distribution that are highly monodispersed	Expensive, time-consuming synthesis procedure, and high temperature	(Ajinkya et al., 2020)
Microemulsion	3.5 ± 0.6	0.0294	Possible to create monodispersed nanoparticles with diverse morphologies	Ineffective and difficult to scale up	(Vidal-Vidal, Rivas and López-Quintela, 2006)
Hydrothermal synthesis	39 ± 5	0.0164	Generating particles with a narrow size distribution that are highly monodispersed	Required high temperature and pressure	(Daou et al., 2006)

2.4   Research Gap

Even though the existing technologies such as thermal decomposition and hydrothermal methods are able to produce MNPs with good monodispersity, there are still few drawbacks associated to these production routes. High temperature and pressure are always the common shortcomings of the synthesis method to produce highly monodisperse MNPs. In addition, high temperatures and pressure will come along with higher cost and safety consideration during the operation. Therefore, it is desirable to seek for a better alternative route to produce highly monodispersed MNPs for application purposes.

Besides the four synthesis methods tabulated in Table 2.2, the grafting of as-synthesized MNP solid powder by using polyelectrolyte to produce polyelectrolyte-functionalized MNP system has gain attention from researchers due to its simple operation, can be conducted in ambient temperature and pressure as well as low cost. The functionalization gives two purposes: (i) to impose functional group onto the MNPs for a specific application, and (ii) to enhance the colloidal stability of MNPs by importing steric hindrance and electrostatic repulsion among MNPs. However, the size of the resulted functionalized MNP clusters is difficult to be controlled, those, the polyelectrolyte functionalization often produces MNP clusters (with a number of MNPs tagged together by polyelectrolyte) with different size. Therefore, it is crucial to segregate the MNPs according to their size after the functionalization, to obtain several fractions of MNPs with lower polydispersity and uniform size. In this regard, LGMS has been proposed to perform the size fractionation of polyelectrolyte functionalized MNPs, which has been studied by Yeap et al. in 2014. However, LGMS in batchwise mode is being used in this work, which is not convenient to be upscaled for the real time industry applications. In conjunction to this situation, it is proposed to integrate the continuous flow feature into the LGMS system to perform the size fractionation of polyelectrolyte functionalized MNPs, so that this process can be conveniently automated and upscaled for industry use. Yet, this area remains unexplored by the researcher around the globe. The main intention of this study is to fill up the gap by thoroughly investigating the possibility of CF-LGMS in segregating the polyelectrolyte-functionalized MNPs according to size into several fractions with lower polydispersity.

CHAPTER 3

METHODOLOGY

3.1 Flowchart

Functionalization of MNPs under different MNP/PSS mass ratio

Dynamic light intensity (DLS) analysis on functionalized MNP systems

Are colloidally stable MNPs obtained?

No

Yes

Continuous flow size fractionation of MNPs with different flowrate and magnets arrangment

Mathematical modeling to calculate particle size distribution from the size fractionation

Comparison of experiment results with COMSOL modeling results

Are both result consistent?

No

Yes

Thesis writing

Figure 3.1: Flow chart of the project

3.2   Material and Equipment

Table 3.1: Materials used in the experiment

Materials/ Chemicals	Suplier
Iron oxide (III) nanoparticles, Fe_3O_4	Sigma Aldrich
Poly(sodium 4-styrene sulfonate), PSS	Sigma Aldrich
Hydrochloric acid, HCl	Chemiz
Deionised water, DI	

Table 3.2: Equipment used in the experiment

Equipment	Brand	Model number
Magnet	-	-
Sonicator bath	Elmasonic	S 180H
End-to-end rotator	SLA Advanced Technology	MX-RL-E
pH tester	EUtech Instrument	PC2700
Centrifuge machine	Eppendorf	Centrifuge 5430
Dynamic light scattering machine (DLS)	Malvern Panalytical	Zetasizer lab
Scanning electron microscope	Joel microscope	JSM-7610F
Peristaltic pump	-	-

3.3   Functionalization of Magnetic Nanoparticles

At first, 0.0625 g of Fe_3O_4 MNPs powder was measured and dispersed in 25 mL of deionized water (DI) water to produce 2.5 g/L concentration of MNPs solution and put inside a centrifuge tube. Simultaneously, 0.0625 g of PSS powder was measured and

dispersed in 25 mL of DI water to produce the same concentration of 2.5 g/L PSS solution in another centrifuge tube. Then, both centrifuge tubes with the solution were fully immersed in a sonication water bath which was then subjected to ultrasonication for 60 minutes. The purpose of this sonication is to aid in the dissolution of MNP as well as PSS and to encourage effective dispersion of the polymeric solution.

After the ultrasonication, the pH values of both MNP and PSS solutions were adjusted to 3.0-4.0 by adding in 1 M of hydrochloric acid (HCl) prior to mixing both solutions. In order to maximise the physisorption of PSS on MNPs via electrostatic attraction after mixing them, the pH adjustment is necessary to guarantee that both MNPs and PSS are carrying opposing charge prior to the functionalization process. Following the mixing of the MNP and PSS solutions, physisorption was allowed to occur for one day in an end-to-end rotating rack with a 50 rpm rotation speed. After a sufficient period for functionalization, PSS-functionalized MNP produced under MNP/PSS mass ratio of 1:1 was produced.

Next, the PSS-functionalized MNP solution subjected to centrifugation in a centrifugal machine (Centrifuge 5430) under 4000 rpm for 60 minutes. After the centrifugation was completed, the precipitated MNPs were held using a magnet when the supernatant with excess PSS was drained out of the centrifuge tube. Then, the precipitated MNPs were resuspended in 50 mL of DI water and ultrasonicated for 20 minutes. To ensure that all of the extra PSS was thoroughly washed out of the solution, this washing procedure was done three times. The washing process is crucial because the presence of excess PSS in the solution stimulates the aggregation of the PSS-functionalized MNP clusters into bigger agglomerates, which subsequently decreases the colloidal stability of the resulting MNP systems. After all, the PSS-functionalized MNPs were kept under ambient temperature for further experimental uses.

All the steps above were repeated to produce PSS-functionalized MNP under different MNP/PSS mass ratios. The mass of MNPs and PSS required for each experiment are shown in **Table 3.3**.

Table 3.3: Mass ratio data of MNPs and PSS

Sample	Mass of MNPs	Mass of PSS	Mass ratio
1	0.0625	0.03125	1:0.5
2	0.0625	0.0625	1:1
3	0.0625	0.125	1:2
4	0.0625	0.25	1:4

3.4   Sedimentation Kinetics of MNPs under Gravitational Field

One of the straightforward investigations performed to ascertain the size of MNPs in the suspension is the sedimentation kinetics test in a gravitational field. Sedimentation refers to the process by which particles suspended in water settle to the bottom as a result of gravity. By this way, the settling time of the MNPs in the suspension can be identified by comparing with different samples. There are two sedimentation tests done during the functionalization of the MNPs with PSS to determine the best choice of the ratio of MNPs to PSS as mentioned on the **Section 3.3**. It is called sedimentation when particles suspended in water settle to the bottom of a glass jar or other container due to the force of gravity. The prepared samples were in concentration of 1000ppm. The initial interval between each photo taken is 5 minutes and further increased to 30 minutes and finally with 1 hour interval. The sedimentation test is stopped when a clear layer of liquid (supernatant) is formed.

3.5   Hydrodynamic Diameter Measurement of Functionalized Magnetic Nanoparticles by Dynamic Light Scattering (DLS)

Photon correlation spectroscopy, or quasi-elastic light scattering, are other names for the same technique, dynamic light scattering (DLS), which uses the Brownian motion of macromolecules in solution to get information, which originates from bombardment by molecules in the solvent, to determine particle size. The temperature, viscosity and

the size all have an impact on the mobility of macromolecules. Furthermore, as the viscosity of the solvent varies with temperature, understanding the precise temperature is crucial for DLS measurements. Large particles diffuse slowly, resulting in comparable positions at multiple time points, but small particles diffuse quickly, resulting in no distinct position. Thus, the information about the size of macromolecules can be gained by tracking their motion over a period of time (Stetefeld et al., 2016).

The dynamic light scattering (DLS) experiment requires monochromatic incoming light, often provided by a laser, to interact with a fluid containing tiny particles in Brownian motion. As a result, when particles with sizes sufficiently small relative to the wavelength of the incident light are present, the Rayleigh scattering process causes the incident light to be diffracted in all directions with wavelengths and intensities that change as a function of time. Light scattering patterns are significantly associated with particle size distributions, therefore by computationally analyzing the spectral features of the scattered light, size-related information of the sample can be obtained (Raja & Barron, 2022).

Direction of incident light
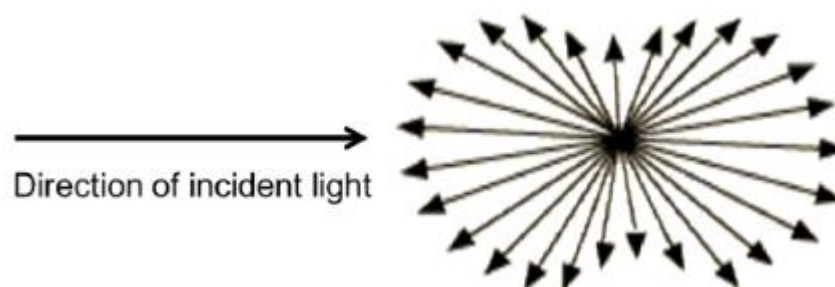
Figure 3.2: Scheme of Rayleigh scattering.

In this investigation, dynamic light scattering (DLS) (performed with a Malvern Instruments Zetasizer ZS) was utilised in order to ascertain Fe_3O_4's hydrodynamic size, denoted as d_H. The diluted concentration of 5–10 mg/L was used for all of the DLS measurements. This was done so that multiple scattering effects and particle interactions could be avoided. In this research, an autofitted exponential decay correlation function was used to identify variations in incoming light intensity scattered back from 173° by nanoparticles. The Cumulants technique, as described in ISO 13321 and ISO 22412, is used mathematically to this correlation function to derive

a translation diffusion coefficient. This translation diffusion coefficient is then afterwards inserted into the Stokes-Einstein equation. Because of this, it is presumed that the shape of any individually dispersed particles or clusters of particles present in the samples is that of a sphere (Yeap et al., 2014).

3.6 Size Fractionation of Magnetic Nanoparticle by Continuous Flow Low Gradient Magnetic Separation

The MNP systems with the greatest colloidal stability (as synthesis by following the procedure in Section 3.3) is used as the model system to experimentally study the effect of flowrate and magnet configurations on the monodispersity of magnetic nanoparticle systems fractionated byperformance of CF-LGMS in fractionating the MNPs. **Table 3.4** shows the manipulation details of all experimental sets being carried out for this studyon the CF-LGMS. There are a total 6 sets of experiments undergone being conducted to investigate the influence of these variables factors on the effectiveness of CF-LGMS in size fractionation resulton MNPs.

At first, 100 ppm mg/L of functionalized MNPs (functionalized under 1:1 ratio of MNPs to PSS ratio of 1:1) feed was prepared from 1000ppm 1000 mg/L of feedstock solution. Then, DI water was used to fill up all the columns before introducing the MNPs solution. This is to ensure the uniform distribution flow of the MNPs that entered the separation columns . After all the columns were completely filled with DI water, the input was then changed to MNPs solution and the stopwatch was started immediately to record the duration of the MNP fraction experiment. After 10 minutes later, the inlet solution was changed switched back to DI water to ensure that the MNPs passed through all of the columns to complete the size fractionation process. Subsequently, the MNPs in each column as well as the effluent solution are recollected in a glass container for preparation of further analysis (sedimentation andby using DLS technique). In addition, the concentration of the result sample in each columneffluent from the CF-LGMS system was determined by using the UV-VIS vis spectrophotometertechnique. The Ssteps above were repeated for different manipulations experimental sets with details as specified in **Table 3.4**. In addition,

Figure 3.3 show the demonstration of the different magnet arrangement used in the experiment which are single side, single pair as well as the dual pair of magnet.

Table 3.4 The details of all experimental set for size fractionation of MNPs by using CF-LGMS technique

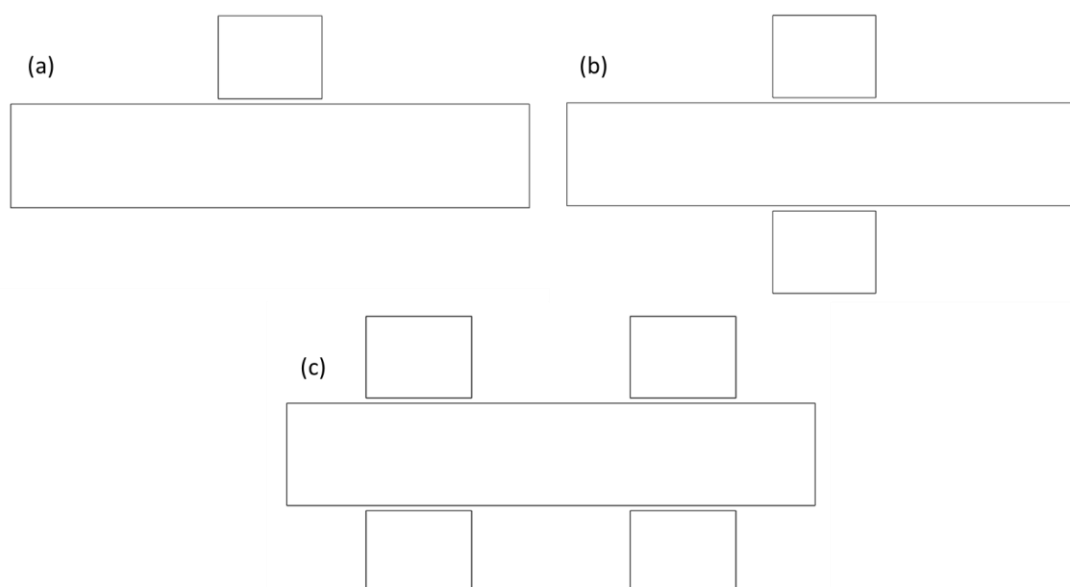| Experiment Set	Flowrate (ml/min)	Magnet Configuration
1	5	Single pair
2	10	Single pair
3	15	Single pair
4	30	Single pair
5	10	Dual pair
6	10	Single side

Figure 3.3: Magnet Configuration demonstration: (a) Single side, (b) Single pair, (c) Dual pair magnet arrangement

In addition, the separation efficiency of a method is determined by how well it removes a certain component from a mixture. It is the ratio of how much of the target component

was recovered during the separation process to how much of that component was originally present in the mixture. Simply said, it quantifies how well one separation method is in removing the desired component while leaving behind any impurities. When the efficiency of the separation process is high, it means that the process is working well; when it is low, it may be necessary to make adjustments. In the experimental section, the concentration of the outlet solution will be measured. After that, the separation efficiency will be calculated using the equation (17) below. It is calculated by the difference between initial concentration and the outlet concentration divided by the initial concentration and multiplied by the 100%.

$$Separation\ Efficiency\ (\%) = \frac{c_O - c}{c_O} \times 100\% \qquad (17)$$

3.7 Simulation of Size Fractionation of Magnetic Nanoaprticles in CF-LGMS System by using COMSOL Multiphysics

When modeling and simulating physical systems, especially those with coupled physics processes like fluid dynamics, structural mechanics, electromagnetics, and heat transfer, COMSOL is a useful tool. In order to comprehend the complex relationship between various physical processes in real-world systems, multiphysics models are required. Research, optimization, and the design of complicated systems are common applications for it in both the academic and business sectors. Thus, it is employed in this research to simulate the CF-LGMS process as mentioned above. The particle tracing module of COMSOL was used to accurately forecast the flow behaviour of MNPs under magnetic field gradient inside the column using the continuous flow technique. The particle tracing method is used to calculate the motion of individual particles by computing their equations of motion in time. Instead of solving for a continuous field, the particle tracing technique in the COMSOL Multiphysics® software solves for a number of distinct trajectories which is in contrast to the majority of the other methods (Track charged particles and particles in fluid flow with simulation , nd).

On the other hand, the simulation of magnetic field produced by the handheld magnet is employing the Magnetic Field Interface. Its primary function is to determine the distributions of the magnetic field and induced currents in and around coils, conductors, and magnets. The magnetic field potential, and in the case of coils, the scalar electric potential, serve as the dependant variable in this physics interface for solving Maxwell's equations. (Software for simulating static and low-frequency electromagnetics , nd).

The study consists of two steps to compute the simulation of the CF-LGMS. First step is stationary simulation of the magnetic field produced by the magnets inside the separation column. Second step is to study the particle tracing for fluid flow to simulate the behavior of MNPs according to magnetic force due to the magnetic field as well as the viscous drag force due to the magnetophoresis. After the simulation, the results are extracted to be compared with the experimental results in order to determine the feasibility of the CF-LGMS. Before conducting the simulation, the column as well as the magnet will be simulated according to the setup of the experiment to ensure the accuracy of the results. The setup of the simulation is as follows as shown in **Figure 3.3.** At first, the geometry of the magnet and the separation column will be built according to the dimensions stated. Then, the magnetic field module used to simulate the magnetic field gradient induced by the magnet inside the separation column. After that, the particle tracing for fluid flow module used to simulate the flow of the MNPs inside the columns. Two forces are acted on the MNPs which are the magnetic force as well as the viscous drag force. These forces are inserted to simulate the CF-LGMS process. Also, the wall condition of the inlet, boundary and the outlet are also controlled to perform the simulation. After all, the simulation will be conducted according to the manipulated variables stated in Table **3.4.** Next, the separation efficiency will be determined by dividing the amount MNPs separated by the inlet amount.
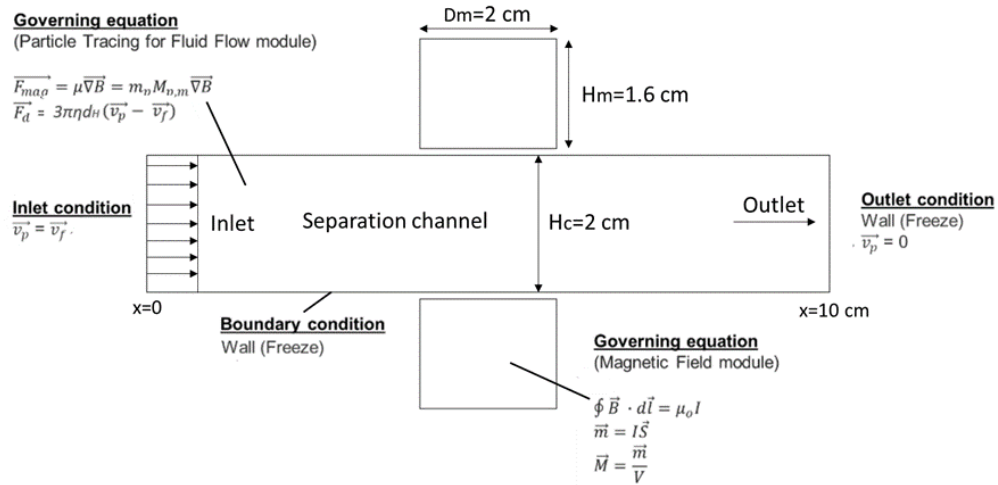
Figure 3.4: Modeling design for CF-LGMS model simulation in 2-dimensional space.

To determine the particle size distribution, the simulation will identify the separation percentage of MNPs based on their hydrodynamic size within a range of 100nm to 600nm, under different manipulation conditions. The percentage of MNPs in the inlet within the specified size range will then be calculated using the size distribution obtained from the DLS result. The amount of MNPs separated in the first column will be calculated by multiplying the separation percentage and the inlet percentage of MNPs of the same size. The percentage of MNPs separated in the first column will then be subtracted from the inlet percentage that enters the second column, and the amount of MNPs being separated in the second column will be determined using a similar calculation based on the reduced inlet percentage. The MNPs separated in the third column will be determined by following the same procedure. Subsequently, the percentage of separated MNPs in each column within the specified particle size range can be plotted to obtain a particle size distribution curve. But there is an additional step which is the normalization of the size distribution curves. This is because the experimental results that send for DLS testing were fixed at a concentration (20 ppm). This normalization process will standardize the curves to the same concentration, enabling comparable size distribution curves to be obtained based on the simulation.

CHAPTER 4

RESULT AND DISCUSSION

4.1   Functionalization of Magnetic Nanoparticles

First, different mass ratios of MNPs to PSS were prepared to study the effect of the amount of PSS supplied during the MNP functionalization process to the colloidal stability of the functionalized MNPs. All the MNP functionalization experiments were conducted under pH 3~4. During the functionalization, the PSS molecules were coated in the surface of the MNPs, which are acting as physical barrier and impose electrostatic repulsion among the functionalized MNP to prevent them from clustering together. Here, the colloidal stability of the functionalized MNPs was determined by measuring the hydrodynamic size (using DLS technique) as well as observing the sedimentation profiles under the gravitational field. The particle size distribution of the functionalized MNPs produced under different MNP to PSS mass ratios are shown in **Figure 4.1** whereas **Figure 4.2** tabulates their respective average hydrodynamic size.

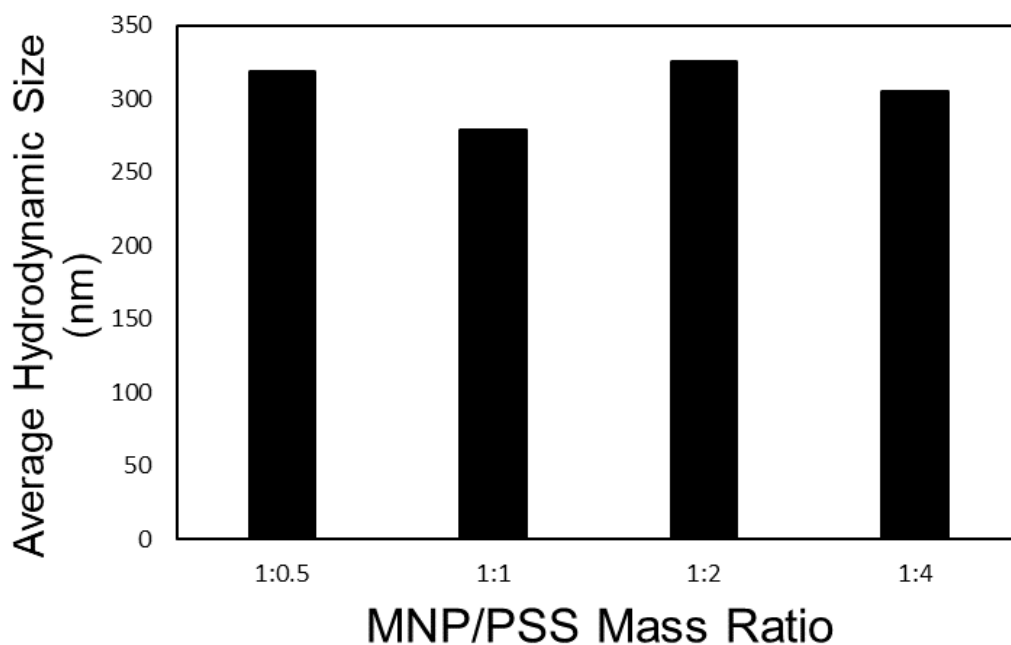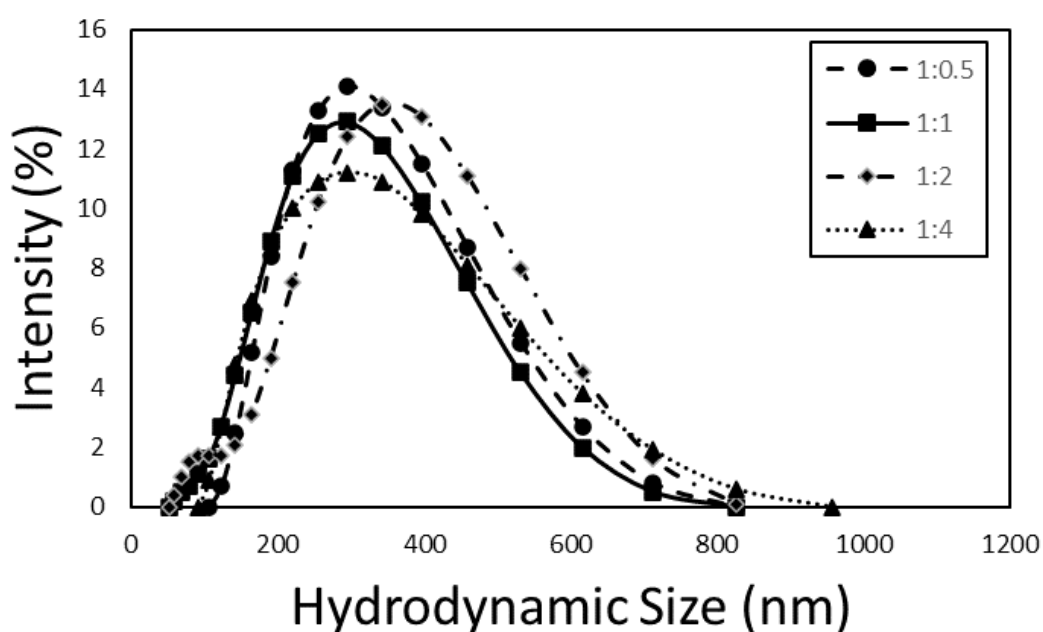**Figure 4.1: Average hydrodynamic of different mass ratios of MNPs to PSS**

Figure 4.2: Size distribution of different mass ratios of MNPs to PSS

According to the result of DLS analysis (**Figure 4.1**), it can be observed that the average hydrodynamic size of MNPs functionalized with MNP to PSS mass ratios of 1:0.5, 1:1, 1:2, 1:4 are given by 293, 223.6, 320.1 and 248.3 nm respectively. The

hydrodynamic size of the particles can be linked to the colloidal stability of the suspension, in which the smaller hydrodynamic size implies the higher colloidal stability of the functionalized MNPs. By definition, the term "colloidal stability" is used to describe a suspension's capacity to prevent particles from agglomerating and settling out from the solution together. In this context, the repulsive and attractive forces between the particles and the energy needed to overcome them to induce aggregation are the determining factors that govern the colloidal stability of a suspension system. Hydrodynamically small colloidal particles are more likely to experience Brownian motion and come into contact among each other at a high frequency to induce aggregation. Despite of that, their colloidal stability can be improved through generating a repulsive force among the particles which aids retain them dispersed (either electrostatic or steric stabilization or both of them). Typically, the colloidally unstable particle systems will show a larger hydrodynamic size, as they tend to clump together to form aggregate due to the overwhelming attractive forces among the particles, which subsequently causes the sedimentation to occur rapidly under the gravitational field. Thus, according to Figure 4.1, the MNP to PSS mass ratio of 1:1 is the optimum ratio to perform the MNP functionalization that gives rise to the functionalized MNP with the highest colloidal stability, as it shows the lowest hydrodynamic diameter (223.6 nm) among all functionalized MNP systems produced in this study. Under the MNP to PSS mass ratio of 1:0.5, the PSS molecules supplied might not be sufficient to fully functionalize the MNPs available in the solution, which causes the functionalized MNPs resulted under this condition to exhibit lower colloidal stability with relatively higher hydrodynamic size at 293 nm. On the other hand, if the PSS is over supplied during the functionalization process (at MNP to PSS mass ratio of 1:2 and 1:4), there will be greater number of PSS adsorbed on the MNP surface, the PSS chain will become compressed to the surface which produced long PSS loops. The long PSS loops extending into solution from the MNP surfaces will be further adsorbed with adjacent particles to form bridges and thereby result in increasingly larger flocs with higher hydrodynamic size and reduced colloidal stability. In addition, the amount of PSS available for the MNP functionalization grows as PSS concentration grows.

Besides, **Figure 4.2** shows the particle size distribution of the MNPs functionalized under different MNP to PSS mass ratios. According to the results, the

MNP system functionalized under MNPs to PSS mass ratio of 1:1 shows the most narrow size distribution and smaller size as compared to the others. Meanwhile, the MNP system functionalized under MNPs to PSS mass ratio of 1:2 shows the broadest particle size distribution. Larger particle size distribution indicates that there is a broad range of particle size in the suspension with the higher degree of polydispersity. These results are consistent with the average hydrodynamic size as tabulated in Figure 4.1. Even through the hydrodynamic size of MNP systems functionalized under MNP to PSS mass ratio of 1:1 and 1:4 are quite similar (which are given by 223.6 nm 248.3 nm, respectively), however, the overall colloidal stability of the MNP system produced under MNP to PSS mass ratio of 1:1 is higher due to the narrow particle size distribution. In fact, the MNP system produced under MNP to PSS mass ratio of 1:4 has a greater portion of larger MNP clusters that are subjected to more rapid sedimentation and exhibit lower colloidal stability. As a result, the MNP system functionalized under MNP to PSS mass ratio of 1:1 demonstrates a better colloidal stability due to the smaller hydrodynamic size and relatively narrower size distribution, which is chosen as the model system to be used in the subsequent study.

Moreover, the sedimentation experiment of the MNP systems functionalized with different MNP to PSS mass ratios were also conducted to further verify the results obtained from the DLS measurement, which are shown in **Figure 4.3**. This sedimentation profile was captured and recorded for a total duration of 5 days (1:4, 1:2, 1:1 and 1:0.5 from the left to right). It is crystal clear that the observation on sedimentation profiles of the functionalized MNPs is basically consistent with the results obtained from the DLS measurement (Figure 4.1 & Figure 4.2). For example, it can be observed that the MNPs functionalized with MNP to PSS mass ratio of 1:1 demonstrated most excellent colloidal stability as the MNPs were not entirely settled down after 5 days of sedimentation, as indicated by the slightly yellowish colour of the solution. On the other hand, the other functionalized MNP samples have shown crystal clear colour after 5 days of sedimentation, which indicates almost all MNPs have been completely settled out of the solution.
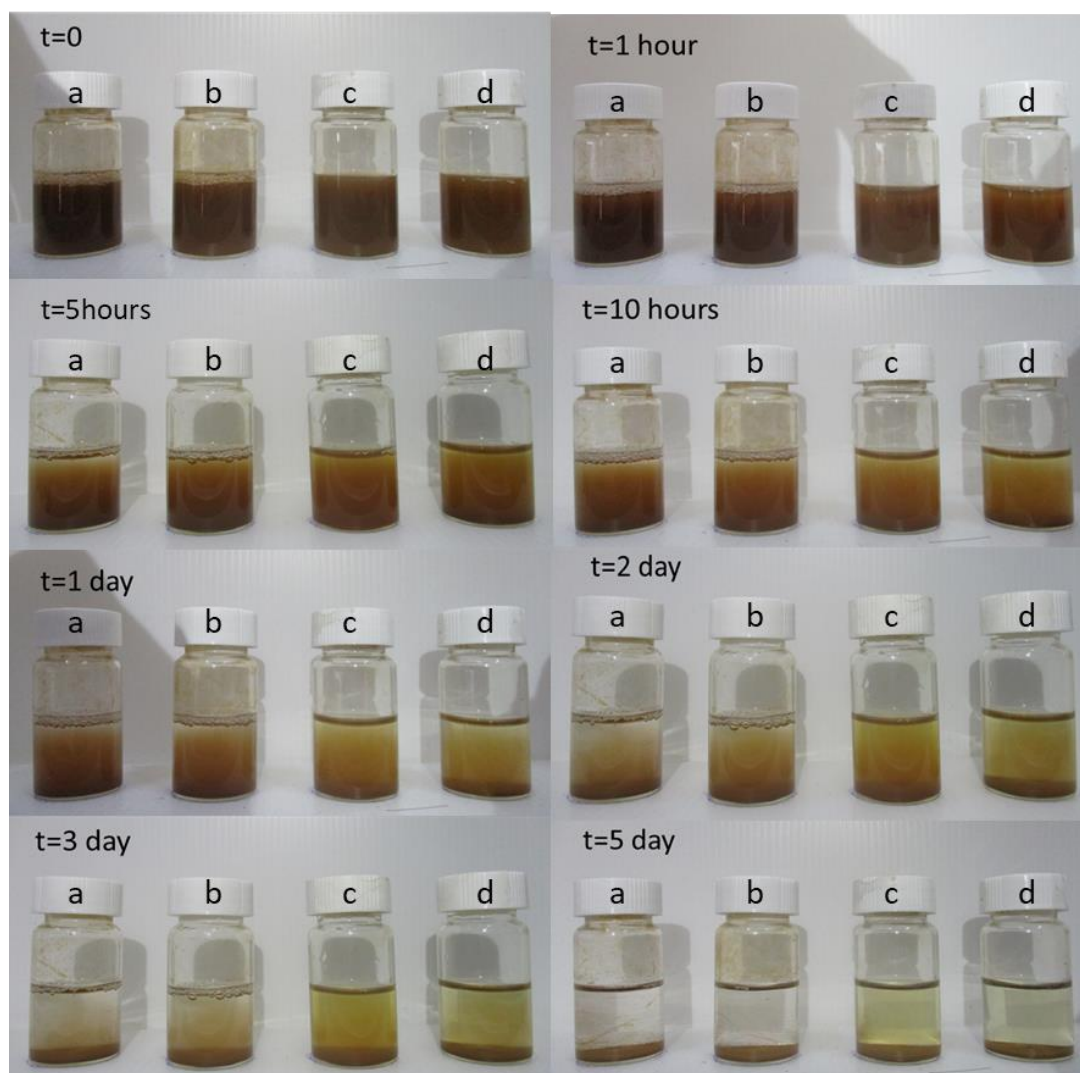
Figure 4.3: The sedimentation profiles of MNP systems functionalized with different mass ratio of MNPs to PSS: (a) 1:4, (b) 1:2, (c) 1:1, (d) 1:0.5

4.2 Continuous Flow Low Gradient Magnetic Separation

In this section, the functionalized MNPs were segregated according to their size by using continuous flow low gradient magnetic separation (CF-LGMS) technique. Here, the functionalized MNPs are channeled into the CF-LGMS system that consists of three columns connected in series arrangement and the MNPs retained in each column are collected and examined. The MNPs system employed in this experiment was functionalized under MNP to PSS mass ratio of 1:1 due to the highest colloidal stability exhibited by the MNP system produced under this condition (see **Section 4.1**).

4.2.1 Feasibility of Continuous Flow Low Gradient Magnetic Separation in the Size Fractionation of Magnetic Nanoparticles

First of all, the results of one experimental set of size fractionation of MNPs by using CF-LGMS technique is thoroughly presented and explained in this subsection, to give an overview on the feasibility of the CF-LGMS process in performing size fractionation of MNPs. In this experiment, the MNP solution at concentration of 100 mg/L was pumped through the CF-LGMS consisting of three columns at a flowrate of 10 mL/min for a period of 10 minutes. Subsequently, the MNPs retained in each column were collected and transferred into a glass container for subsequent analysis by using various techniques such as UV-Vis spectrophotometry, DLS measurements, and sedimentation test. The hydrodynamic sizes and size distribution of the MNPs captured in each column using CF-LGMS were determined by using DLS, and the results are illustrated in **Figure 4.4** and **Figure 4.5**.
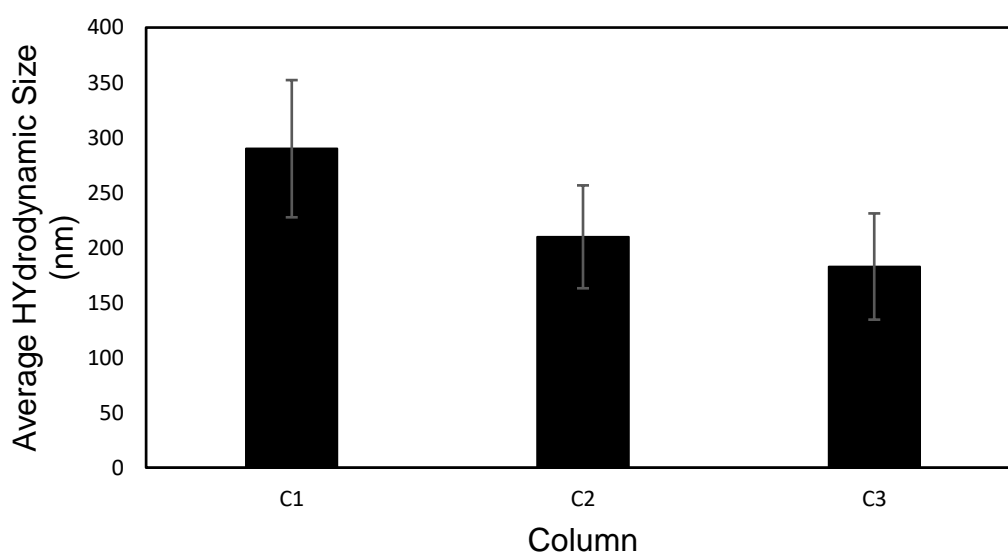

Figure 4.4: Hydrodynamic Size of MNPs in different columns at 10 ml/min
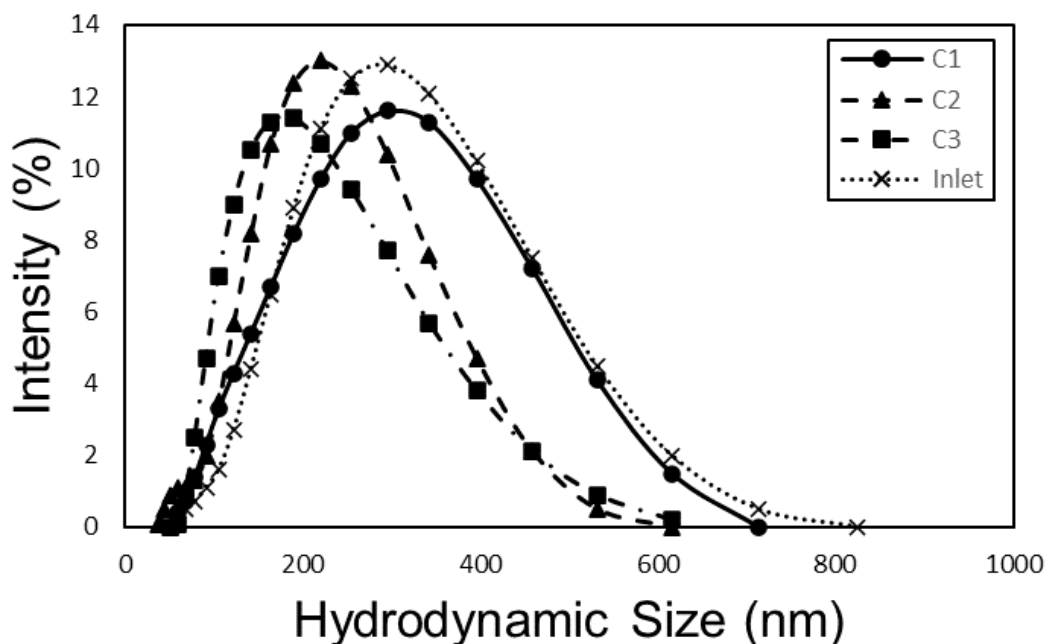
Figure 4.5: Size distribution of MNPs in different columns at 10 ml/min

Based on the DLS measurement results depicted in **Figures 4.4** and **4.5**, there is a decreasing trend in the hydrodynamic size of MNPs from the first column to the third column. For instance, the average hydrodynamic size of MNPs in the first column is 289.9 nm, followed by 209.8 nm in the second column and 182.8 nm in the third column. These results demonstrate the success of the size fractionation of MNPs in different columns through the CF-LGMS technique.

Theoretically, the separation of MNPs in this CF-LGMS experiment will result in the largest MNPs being separated in the first column, intermediate-sized MNPs retained in the second column, and smaller MNPs fractionated in the third column. This is due to the fact that the larger MNPs will experience greater magnetic forces than smaller ones under the same magnitude of magnetic field gradient, as stated in equation (3) in **Section 2.2**. According to equation (3), the magnetic force is proportional to the mass, and hence the size, of the MNPs. As the MNPs flow through the first column, the larger MNPs will experience the higher magnetic force under the magnetic field imposed by the magnets around the column. Consequently, larger MNPs could be successfully attracted toward the wall of the column adjacent to the magnets, while smaller counterparts may escape from being captured and flow to the

subsequent column. As the solution flows into the second column contains a generally higher portion of smaller-sized MNPs, the MNPs that are separated and retained in the second column are smaller in size overall. In fact, the experimental results are consistent with theoretical expectations, as the MNPs recollected in the first column are showing the largest hydrodynamic size (289.9 nm), and those collected in the third column has the smallest ones (182.2 nm).

In addition, **Figure 4.5** also shows that the size distribution of the MNPs retained in the three columns is showing a decreasing trend in the particle size range as going from the first to the third columns. Typically, MNPs in the first column have the larger particle size, as evidenced by the bell-shaped size distribution curve that is skewed towards the right side of the graph. Conversely, the size distribution curve of the MNPs separated in the third column leans towards the left side of the graph which is indicating the smaller particle size, whereas the MNP fraction retained in the second column is fallen in between. As the size distribution curve of the inlet stream has a wider range, the purpose of the CF-LGMS is to narrow down the size distribution of the MNPs separated in the three columns. It is obvious that the size distribution of the MNPs in the second column and third column are becoming narrower as compared to the inlet.

Determining the viability of CF-LGMS in size fractionation of MNPs requires examining not only the average size and size distribution of the MNP fractions maintained in all columns, but also the degree of monodispersity. By definition, the degree of monodispersity refers to how uniform the particles are in size and shape within a sample. The term "dispersity" is used to describe the variety of particle sizes and shapes present in a given sample, with "monodisperse" samples containing particles that are uniform in size and shape, and "polydisperse" samples containing particles of varying sizes and shapes. As outlined in **Section 2.3**, there are several parameters to determine the degree of monodispersity of a particle system, such as standard deviation and the polydispersity index (PDI), and the parameters of the MNP fractions resulted in this CF-LGMS experiment are presented in **Table 4.1**.

Table 4.1 indicates that the standard deviations of the MNP fractions retained in the first to third column are given by 124.7, 93.53, and 96.56 nm respectively. It is evident that the standard deviation of the MNP fractions decreases from the first to the

subsequent columns. The degree of variability in a dataset is measured by its standard deviation, which represents the numerical measure of the spread of data points around the set's mean. In general, it indicates how far each data is from the mean of the sample data. A high standard deviation corresponds to values that are widely dispersed from the mean, while a low standard deviation corresponds to values that are tightly clustered around the mean. When comparing the two curves, the curve with a smaller standard deviation has a sharper peak and narrower spread, while the one with a larger standard deviation is flatter and more widely distributed (Bhandari, 2023). For example, the size distribution of the MNPs collected in the third column can be represented as (182.8 ± 96.56 nm), indicating that the particle size of the MNPs ranges from 279.36 nm to 86.24 nm with a mean diameter of 182.8 nm. This trend is also consistent with the results obtained in the size distribution curves. When the curves get narrower, the standard deviation also reduces. However, the slight increment in the standard deviation in the third column may be attributed to some of the MNPs becoming larger clusters.

Moreover, the polydispersity index (PDI), which can be calculated from the standard deviation using equation (16) in **Section 2.3**, is another important parameter to determine the degree of monodispersity in the sample of particles. As shown in **Table 4.1**, the PDIs of the MNPs retained in the first column to the third column are given 0.1850, 0.1987, and 0.2791, respectively. The PDI is related to the standard deviation and monodispersity in that it measures the distribution width of particle sizes relative to the mean particle size. According to Sadeghi et al. (2015), a suspension can be considered monodisperse if the PDI value is less than 0.3 and has a single peak in the size distribution curve (Sadeghi et al., 2014). Thus, since the PDIs of all MNP fractions retained in the three columns are lesser than 0.3, it can be concluded that the MNP fractions segregated by CF-LGMS process are monodisperse. The PDI values increment from the first column to the third column can be due to the average hydrodynamic size. This is because according to the equation (16), the PDI is found by dividing the square of the standard deviation by the MNPs' average particle size. Consequently, when the average hydrodynamic size is large, the resulting PDI value will be decreased if the standard deviation has small decrement. Therefore, this can explain why the PDI values increased from the first column to the third column.

Table 4.1: Degree of Monodispersity of MNPs in different column

Column	Average hydrodynamic size (nm)	Standard deviation (nm)	Polydispersity Index (PDI)
1	289.9	124.7	0.1850
2	209.8	93.53	0.1987
3	182.8	96.56	0.2790

As the size fractionation of MNPs by CF-LGMS is considered successful (with the largest MNP fractions obtained in the first column and the smallest MNP fractions obtained in the last column), the effect of two design parameters of CF-LGMS setup (MNP solution flowrate and magnet configuration around the columns) on the effectiveness of MNP size fractionation is investigated in the subsequent subsections.

4.2.2 Effect of Flowrate on the Performance of CF-LGMS in Size Fractionation of Magnetic Nanoparticles

In this subsection, the effect of flow rate of the MNPs solution through the CF-LGMS system on the effective of the MNP fractionation is studied. Specifically, the flow rate was set to 5, 15, and 30 mL/min in these experiments, with the magnet configuration of single pair was being adopted. The resulting particle size distribution of MNP fractions retained in each column were analyzed and compared for all these experiments conducted under different flow rates. This analysis is presented in **Figure 4.6**, which show the particle size distribution of MNP fractions retained in each column for CF-LGMS experiment performed under different flow rates of the MNPs solution.
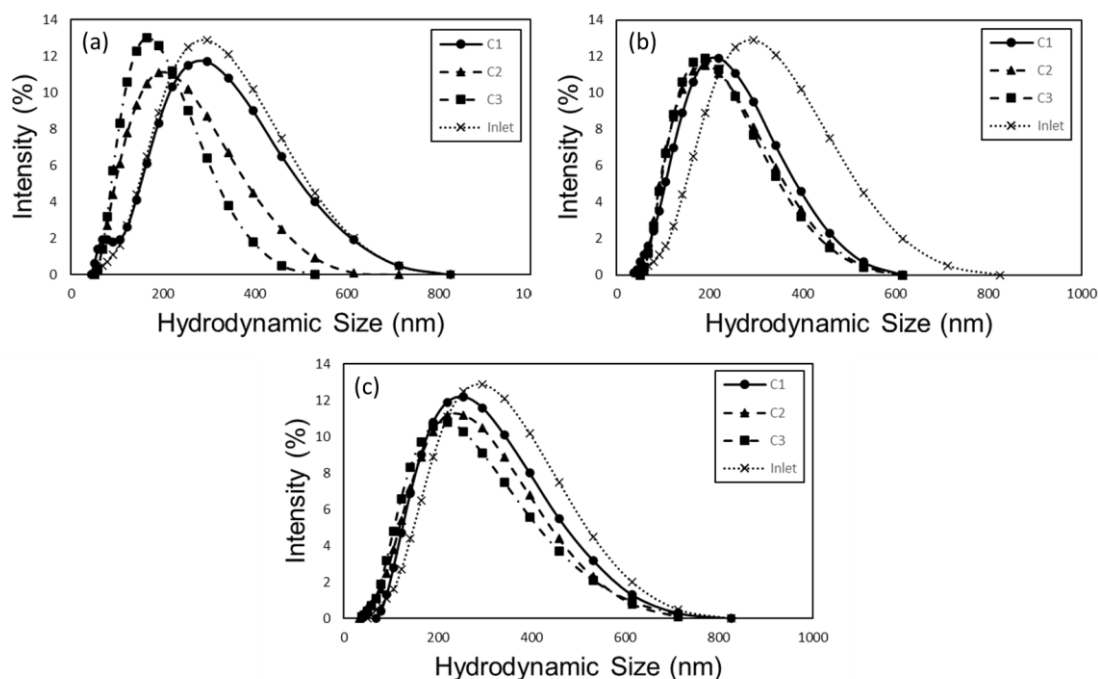
Figure 4.6: Size distribution of MNPs in different columns at different flowrate: (a) 5 ml/min, (b) 15 ml/min, (c) 30 ml/min

Figure 4.6 (a) shows the size distribution of MNP fractions segregated by CF-LGMS conducted at a flow rate of 5 mL/min. As compared to the MNP fractions segregated by CF-LGMS under the flowrate of 10 mL/min (Figure 4.5), the size distribution of MNP fractions resulted in this experiment displays more prominent changes. This is because the time that the MNPs stay in the separation columns, or their residence time, is directly related to the flow rate of the MNPs solution, in such a manner that the lower flow rates lead to the longer residence times. Therefore, for CF-LGMS operated at 5 mL/min, the residence time of MNPs in each column is higher which in turn allows the magnets have more time to attract the a particular MNP in the column. Under this scenario, higher proportion of larger MNPs are captured in the first column, while the remaining MNPs with the smaller size enter the second column. Next, the intermediate-sized MNPs are separated in the second column, and as a result, the MNPs that are flowing into the third column are primarily of smaller size than that being found in the other columns. By looking at the size distribution of MNP fractions

retained in each column, it has been suggested that the size fractionation process by using CF-LGMS technique is more effective if it is conducted at lower flow rates.

In addition, a comparison between **Figure 4.5** and **Figure 4.6 (a)** also reveals a narrowing trend in the size distribution of MNP fractions retained in the second and third columns for CF-LGMS conducted at flowrate of 5 mL/min (see **Figure 4.6 (a)**). This phenomenon also be rationalized by using the residence time of MNPs in the separation columns. At lower flow rates, the larger MNPs are primarily separated in the first column, leaving behind mostly intermediate-to-small MNPs in the remaining solution. As a result, the particle size distribution of MNP fractions retained in the second and third columns becomes narrower due to the restricted range of particle sizes that is supplied to them. The MNP fraction in the third column exhibits the narrowest size distribution curve since the size of the MNPs escaping from first and second columns is relatively small (the larger MNPs have been successfully separated in first and second columns). However, the particle size distribution curve of the MNP fraction in the first column for CF-LGMS performed under 5 mL/min (see **Figure 4.6 (a)**) is wider than that of 10 mL/min (**Figure 4.5**). This is because excessive residence time may have an adverse effect on the separation process. MNPs can undergo irreversible aggregation and form larger clusters as they migrate toward the magnets and exposed to the magnetic field for a prolonged period (Ko et al., 2016). Additionally, the extend of aggregation of MNPs is influenced by their concentration in the solution. At the first column, the concentration of MNPs is the highest and intensive aggregation may occur under low flow rates (with high residence time). Under the high concentration of MNP in the first column, the availability of free particles for aggregation is also high, which subsequently leading to the intense collision frequency and accelerates the entire aggregation process (Yeap et al., 2014).

On the other hand, the particle size distribution of MNP fractions retained in each column for CF-LGMS conducted at higher flow rates show less noticeable differences. In **Figure 4.6 (b)** (flow rate at 15 ml/min) and **Figure 4.6 (c)** (flow rate at 30 ml/min), only a slight shifting of size distribution (towards the left with the smaller size) is observed for the MNP fractions retained in the downstream (second and third columns) as compared to those in the first column. This is attributed to the shorter residence time of the MNPs in each separation column. At higher flow rates, the

velocity of MNPs increases, leading to the shorter residence time of a particular MNP in the columns. Consequently, MNPs have less time to be separated and retained in a particular column, resulting in a larger number of unseparated MNPs being flushed out of the column and flowing to the subsequent column(s) (Tan et al., 2022). Therefore, a higher proportion of the larger MNPs could be escaped from the upstream column and flow into the second and third columns, causing the MNP fractions retained in all columns to exhibit the similar size distribution.

Apart from the size distribution, a comparison of the average hydrodynamic size of MNP fractions retained in different separation columns of CF-LGMS system conducted at various solution flowrates is demonstrated in **Figure 4.7**. The results indicate that the CF-LGMS operated under the lowest flowrate (5 mL/min) gives rise to more distinguish differences in the hydrodynamic size of MNP fractions retained in each separation columns, as compared to those operated under the higher flowrates (15 mL/min and 30 mL/min). For instance, at a flowrate of 5 mL/min, the average hydrodynamic size of MNP fractions retained in the first column is 244.1 nm, followed by 191.6 nm in the second column and 158.2 nm in the third column. However, at a flowrate of 15 mL/min, the average hydrodynamic size of MNP fraction retained in the first column is 197.7 nm, followed by 183.3 nm in the second column and 170.4 nm in the third column. Finally, at a flowrate of 30 mL/min, the average hydrodynamic size of MNP fraction retained in the first column is 225.8 nm, followed by 209.3 nm in the second column and 198.3 nm in the third column. This is because increasing the flowrate of the MNP solution for the CF-LGMS process results in a shorter residence time for the MNPs in a particular column and separated by the magnets. Consequently, the CF-LGMS conducted under the higher flowrates results in the less pronounced differences in the average hydrodynamic size of the MNP fractions retained in each separation columns. This result is also consistent with the size distribution result (**Figures 4.6 (a)-(c)**) which is suggesting that the difference between the MNP fractions retained in each column is diminishing for CF-LGMS operation conducted at the higher flowrates. In fact, this reduction in differences also corresponds to a decrease in the MNP size fractionation efficiency by using the CF-LGMS technique, in which the MNP fractions with almost the similar size distribution are being collected in all the three columns.
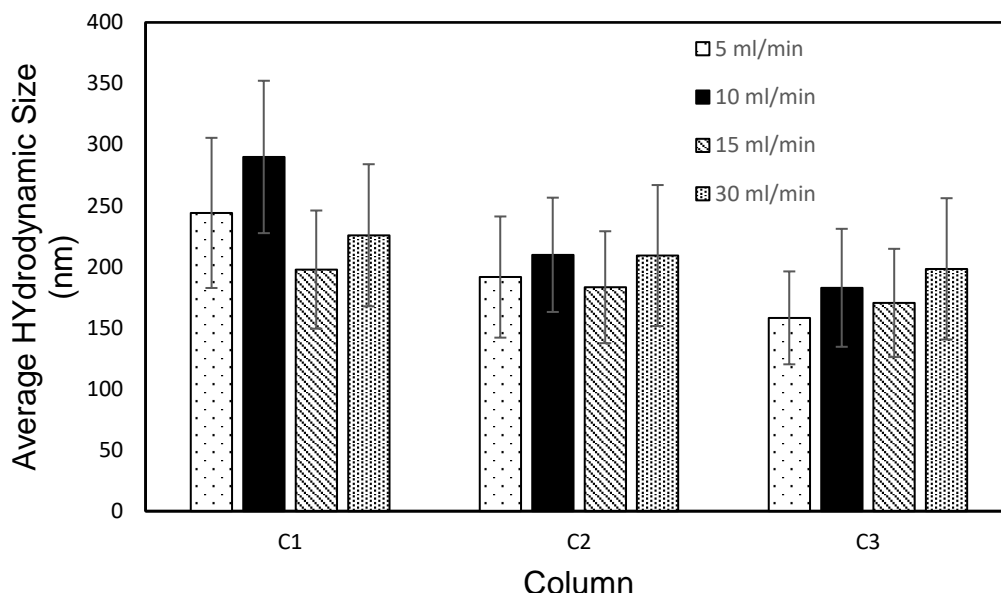
Figure 4.7: Average hydrodynamic size of MNPs collected in each column for CF-LGMS operated at different flowrate

In order to further verify the effect of flowrate on the performance of CF-LGMS technique in the size fractionation of MNPs, the degree of monodispersity of the segregated MNP fractions in different columns is evaluated. As similar to the analysis in the previous subsection, the standard deviation and PDI values are used to reflect the degree of monodispersity of the MNPs, which is tabulated in **Table 4.2**. At a flowrate of 5 mL/min, the standard deviation of the particle size for MNP fractions retained in the first, second, and third columns are 122.9 nm, 99.16 nm, and 76.02 nm, respectively. At a flowrate of 15 mL/min, the given standard deviation value of MNP fractions retained in the first, second, and third columns are 96.69 nm, 91.58 nm, and 88.59 nm, respectively. Finally, at a flowrate of 30 mL/min, the MNP retained in the first column has standard deviation of 116.3 nm, while those in the second column the third column are recorded as115.4 nm and 115.7 nm, respectively. Thus, it is evident that at the lowest flowrate (5 mL/min), there is a significant difference between the standard deviations in term of particle size of the MNP fractions retained in each column. As the flowrate of the CF-LGMS operation increases, the differences in standard deviation between the MNP fractions retained in each column become less

pronounced. In particular, at a flowrate of 30 mL/min, the standard deviation of MNP fractions retained in each column is quite similar.

In addition, the PDI values also provide comparable results on the degree of monodispersity for MNP fractions segregated by the CF-LGMS experiments. At flowrate of 5 mL/min, the PDI values of MNP fractions in the first, second, and third columns are 0.2535, 0.2678, and 0.2309, respectively. At 15 mL/min, the PDI values of MNP fractions in the first, second, and third columns are 0.2392, 0.2496, and 0.2703, respectively. Lastly, at 30 mL/min, the PDI values of MNP fractions in the first, second, and third columns are 0.1609, 0.3026, and 0.4006, respectively. The PDI values at 5 mL/min flowrate indicate that the size fractionation process is excellent as it produces all MNP fractions with PDI below 0.3, which indicates the MNP fractions resulted are considered monodispersed with the fractions at the last column has the lowest PDI value (and hence lowest degree of monodispersity). However, at higher flowrates, the PDI value increases for MNP fractions produced at the more downstream locations. For instance, at 15 mL/min flowrate, the PDI value increases for MNP fractions retained in the first to the third column but the values are still below 0.3. On the other hand, at 30 mL/min flowrate, the PDI values of the MNP fractions increases more dramatically, with the second and third columns having PDI values over 0.3, which implies that the MNP fractions are considered polydisperse.

Up to this stage, it can be concluded that the degree of monodispersity of the MNPs fractionated by using CF-LGMS can be improved by operating the size fractionation process under a lower flowrate. This is because at lower flowrates, larger MNPs has the longer residence time to be separated in the first column, intermediate-sized MNPs can be separated in the second column, and smaller-sized MNPs can be separated in the last column. As a result, the performance of the fractionation process can be boosted if the CF-LGMS is operated under a lower flowrate.

Table 4.2: Comparison of Monodispersity of the separated MNPs at different flowrate

Column	Average hydrodynamic size (nm)			Standard deviation (nm)			Polydispersity Index (PDI)		
	Florate (ml/min)			Florate (ml/min)			Florate (ml/min)		
	5	15	30	5	15	30	5	15	30
1	244.1	197.7	289.9	122.9	96.69	116.3	0.2535	0.2392	0.1609
2	191.6	183.3	209.8	99.16	91.58	115.4	0.2678	0.2496	0.3026
3	158.2	170.4	182.8	76.02	88.59	115.7	0.2309	0.2703	0.4006

4.2.3 Effect of Magnet Arrangement on the Performance of CF-LGMS in Size Fractionation of Magnetic Nanoparticles

In order to further investigate how the design parameters of CF-LGMS affect its effectiveness in performing size fractionation of MNPs, the experiments to segregate the MNPs by using CF-LGMS were conducted under different magnet arrangement. In the previous subsection (to the study of the effect of flowrate on the MNP fractionation efficiency of CF-LGMS), the magnet arrangement is fixed at one pair of magnets placed at the middle of the separation columns. However, in this subsection, the magnet arrangement is serving as the manipulated variable of the experiment and the flowrate is fixed at 10 mL/min for all the experiment, whereas the magnets were manipulated as one side and two pairs. The demonstration of the magnet arrangement is shown in the **Section 3.6.**

The particle size distribution of the MNPs that were retained in different columns with single side of the magnet as well as two pairs of magnets in **Figure 4.8**. Based on **Figure 4.8 (a)**, the size distribution of the MNP fractions collected in the three columns (with single side of magnet) almost overlap among each other. This indicates that the fractionation was not effective under this magnet arrangement, as the hydrodynamic size of the MNP fractions in all columns were identical. For instance,

the average hydrodynamic size of the MNPs from first column to last column under single side magnet are 223 nm, 210.8 nm and 196.9 nm respectively (see **Figure 4.9**). In this context, the decrease in the average hydrodynamic size of MNPs is not significant, with only a 26.1 nm difference between the first and third columns. This is due to less extent of magnetophoresis being induced in the columns, as only one magnet located at single side of the column generates only minor proportion of intense magnetic field gradient within the columns in overall. So, the MNPs are subjected to weaker magnetic force which in turn causes the relatively large MNPs to escape from the upstream column. So, high proportion of the large MNPs will be entering and being captured in the downstream columns. Therefore, the size fractionation of the MNPs by using CF-LGMS under this magnet configuration is not satisfactory.

On the other hand, the use of a dual pair of magnets in the CF-LGMS process results in significant differences in the particle size distribution of the MNP fractions retained in different columns, as compared to the single side magnet arrangement. As depicted in **Figure 4.8 (b)**, the size distribution curve from the first to the third column shows a narrowing trend, indicating the MNP fractions retained in the more downstream column exhibit the higher degree of monodispersity. In fact, the average hydrodynamic size of MNP fractions retained in the first, second and third columns are given by 249.6 nm, 200.6 nm and 167.7 nm, respectively (see **Figure 4.9**). This is because the magnetophoresis of magnetic particles is strongly correlated with the magnetic field gradient (Yeap et al., 2014). Thus, a dual pair of magnet arrangement can provide intense magnetic field strength and gradient throughout the higher proportion of the column of the CF-LGMS setup, which allows the MNPs to experience immense magnetic force in most region of the separation column. For the MNPs that are escaped from the first pair of magnets, they can still be attracted by the magnetic field gradient induced by the second pair of magnets near the outlet of the column. The intense magnetic field throughout the separator column is capable of capturing and separating most of the larger-sized MNPs in the first column. Consequently, smaller-sized MNPs are left to enter the second column, resulting in a decrease in the average hydrodynamic size of MNPs in that column. The third column, under the dual pair magnet arrangement, exhibits a comparatively lower average hydrodynamic size of MNPs than that under the single side magnet arrangement, as the magnetic field is strong enough to capture and separate very small-sized MNPs.

Consequently, the use of a dual pair of magnet arrangement enhances the MNP fractionation efficiency by using CF-LGMS technique.
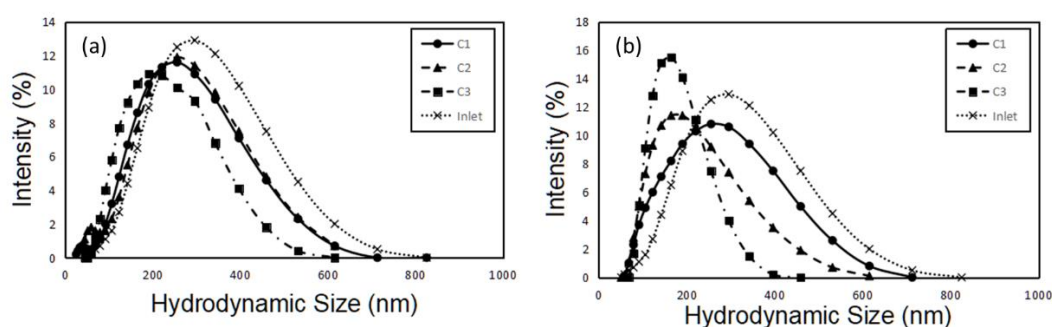

Figure 4.8: Size distribution of MNP fractions retained in the three columns for CF-LGMS of different magnet arrangement: (a) single side magnet arrangement, (b) dual pair magnet arrangement
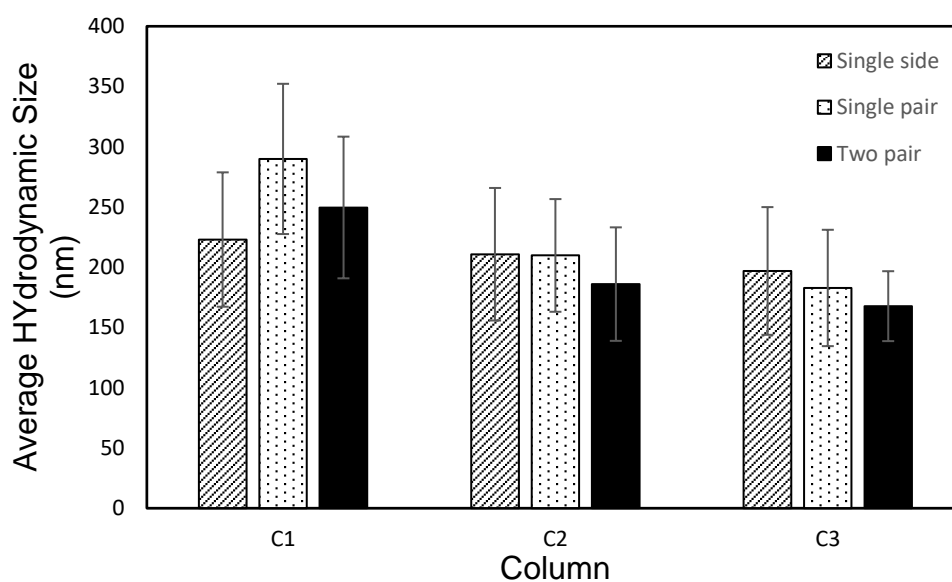
Figure 4.9: Average hydrodynamic size of MNP fractions retained in each column for CF-LGMS of different magnet arrangements.

In addition, **Figure 4.9** demonstrates the average hydrodynamic size of the MNPs across the separation columns under different magnet arrangements. The average hydrodynamic size of the MNPs from first column to last column under single side magnet are 223 nm, 210.8 nm and 196.9 nm respectively. On the other hand, under

dual pair magnet arrangement, the average hydrodynamic size are 249.6 nm, 186.0 nm and 167.7 nm respectively.

As previously mentioned, the magnetic field gradient induced by different magnet arrangements will have an effect on the separation efficiency. Under a dual pair of magnet arrangement, the hydrodynamic size of MNPs in the first column was found to be larger than in the other columns. This can be attributed to the strong magnetic field generated by the four magnets, which is capable of capturing and separating most of the larger-sized MNPs in the first column. Consequently, smaller-sized MNPs are left to enter the second column, resulting in a decrease in the average hydrodynamic size of MNPs in that column. The third column, under the dual pair magnet arrangement, exhibits a comparatively lower average hydrodynamic size of MNPs than that under the single side magnet arrangement, as the magnetic field is strong enough to capture and separate very small-sized MNPs. However, compared to the single side magnet arrangement, the decrease in the average hydrodynamic size of MNPs is not significant, with only a 26.1 nm difference between the first and third columns. These findings indicate that size fractionation of MNPs is not as efficient under the single side magnet arrangement as it is under the dual pair magnet arrangement.

In addition, the MNP fractions' degree of monodispersity can also be characterized by standard deviation and PDI values. When using a single side magnet arrangement, the standard deviations of the MNP fractions retained in the first column to the third column are 111.5 nm, 110.0 nm, and 106.0 nm, respectively. However, under a dual pair arrangement, the standard deviations are 117.6 nm, 94.21 nm, and 58.03 nm, respectively. The standard deviations of the MNP fractions produced by the single side magnet arrangement are almost equal among each other, which indicates that the size distributions of the MNPs are similar across all separation columns, as demonstrated in **Figure 4.8 (a)**. In contrast, the standard deviations across the separation columns under the dual pair magnet arrangement show a decreasing trend, which corresponds to the results shown in **Figure 4.8 (b)**, where the size distribution curves are narrowing from the first column to the third column. Furthermore, the degree of monodispersity of the MNP fractions can also be justified by using PDI values. For the single side magnet arrangement, the PDI values increase from the first

column to the third column with values of 0.25, 0.2723, and 0.2898, respectively. On the other hand, for the dual pair magnet arrangement, the PDI values decrease from the first column to the third column with values of 0.2220, 0.2206, and 0.1197, respectively. Both magnet arrangements exhibit PDI values below 0.3, which indicates a monodisperse particle distribution. However, under single side magnet arrangement, the increasing trend in PDI values is due to the decreasing average hydrodynamic size of the MNPs across the separation columns while the range of the size distribution remains almost constant. Conversely, the PDI value of the MNPs in the third column under dual pair magnet arrangement is much lower than those in the first and second columns. The significant reduction in standard deviation and PDI values for the MNP fractions retained in the downstream columns under dual pair magnet arrangement suggests that it imposes better performance in fractionation as compared to the single side magnet arrangement.

Table 4.3: Comparison of degree of monodispersity of the fractionated MNPs in different columns under CF-LGMS of different magnet arrangement

Column	Average hydrodynamic size (nm)			Standard deviation (nm)			Polydispersity Index (PDI)		
	Magnet Arrangement			Magnet Arrangement			Magnet Arrangement		
	Single side	Single pair	Dual pair	Single side	Single pair	Dual pair	Single side	Single pair	Dual pair
1	223.0	289.9	249.6	111.5	124.7	117.6	0.2500	0.1850	0.2220
2	210.8	209.8	200.6	110.0	93.53	94.21	0.2723	0.1987	0.2206
3	196.9	182.8	167.7	106.0	96.56	58.03	0.2898	0.2790	0.1197

4.2.4   Separation Efficiency of Magnetic Nanoparticles in CF-LGMS Process

The impact of various CF-LGMS process design parameters (magnet configuration and flowrate) on the separation efficiency is examined in this subsection. The recovery of the separated MNPs, as well as how well the method separates them from the sample

matrix, are measures of its separation efficiency. It is a crucial parameter to be studied because it governs the amount of MNPs in the influence that involves in the size fractionation process in the CF-LGMS system without being flushed out of the column. **Table 4.4** tabulates the separation efficiencies of the total 6 sets of CF-LGMS experiments, after going through the three columns in the series arrangement. As the inlet of the MNP solution was fixed as 100 mg/L, the separation efficiency is depending on the MNP concentration of the effluent, which was determined using UV-VIS spectroscopy. Based on the results, the separation efficiencies for CF-LGMS operated with flowrate of 5 mL/min, 10 mL/min, 15 mL/min and 30 mL/min (under single pair magnet arrangement) are given by 83.72%, 69.08%, 56.87% and 38.03% respectively. Whereas, the separation efficiency of CF-LGMS operated with single side and dual pair magnet arrangement (under flowrate of 10 mL/min) are given by 58.03% and 80.45% respectively.

The decline in separation efficiency of CF-LGMS with increasing flowrate of the MNPs solution is due to the shorter residence time of the MNPs in the separation columns, which results in lesser MNPs being captured and separated in the columns. In contrast, when the number of magnets per column is increased (magnet configuration is altered from one side to one pair and then to dual pair), the separation efficiency is also observed to be increased. These findings are consistent with the earlier discussion, wherein the increased number of magnets leads to the higher coverage of more intense magnetic field gradient within the column. For instance, in the dual pair magnet arrangement, four magnets generate high magnetic field gradients near the inlet and outlet of the column, allowing for more MNPs to be separated from the solution. Notably, the experiments conducted at a flowrate of 5 mL/min and using the dual pair magnet arrangement have demonstrated the highest separation efficiencies, exceeding 80% in comparison to other experiment sets. Hence, these two experiment sets can be considered suitable for increasing separation efficiency.

Table 4.4: Separation efficiency of MNPs in different experiment set of size fractionation of MNPs by using CF-LGMS

Experiment set	Concentration (ppm)		Separation Efficiency (%)
	Inlet	Outlet	
1		16.2842	83.71
2		30.9158	69.08
3		43.1263	56.87
4	100	61.9684	38.03
5		41.9684	58.03
6		19.5474	80.45

4.3 Size Fractionation of Magnetic Nanoparticle by using Continuous Flow Low Gradient Magnetic Separation: Theoretical Simulation

In this section, the size fractionation of MNPs by using CF-LGMS technique is modelled and simulated numerically. Then the simulation results are compared with the experimental resulted discussed in the previous section to verify the accuracy of the model.

Figure 4.10 shows the simulation results of magnetic field within a CF-LGMS column employed in the current study by using the COMSOL Multiphysics software. There are a total of three types of magnet arrangement used in this study, which are single side, single pair as well as the dual pair magnet arrangement. As shown in this figure, the region covered by more intense magnetic field (> 0.4 T) increased as the number of magnets increased and this led to the wider coverage of the intense magnetic field inside the separation columns. As a result, the MNPs that enter the separation columns with higher number of magnets will experience higher magnetic field gradient as compared to those magnet arrangements with the lesser number of magnets (single side magnet arrangement).
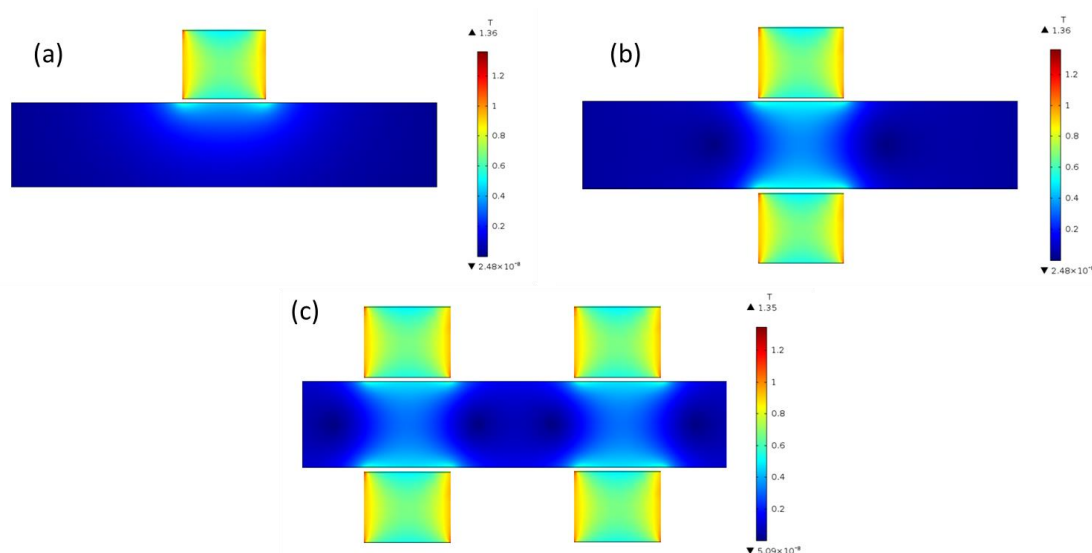
Figure 4.10: Magnetic field simulation result: (a) single side magnet arrangement, (b) single pair magnet arrangement, (c) dual pair magnet arrangement

On the other hand, **Figure 4.11** shows the trajectory of MNPs at different vertical location at the inlet after entering to the separator column, under different flowrate and magnet arrangement, as predicted by the model simulation. Based on the results, when the flowrate increased, the MNPs are being flushed out more rapidly in the horizontal direction and the amount of MNPs being attracted to the wall of the separation column decreases (**Figure 4.11(a)-(d)**). In addition, when the magnet arrangement dual pair is adopted, there are also more MNPs being captured at the wall of the separation columns as the MNPs are experiencing larger magnetic field gradient (and hence stronger magnetic force) that steer them vertically towards the magnets more effectively. The trend shown in Figure **4.11** are consistent with the experimental results which have been reported above and in previous literature (Tan et al., 2022) . Hence, these simulation results can be safely used in the further analysis and discussion of the MNP fractionation process in the following subsections.
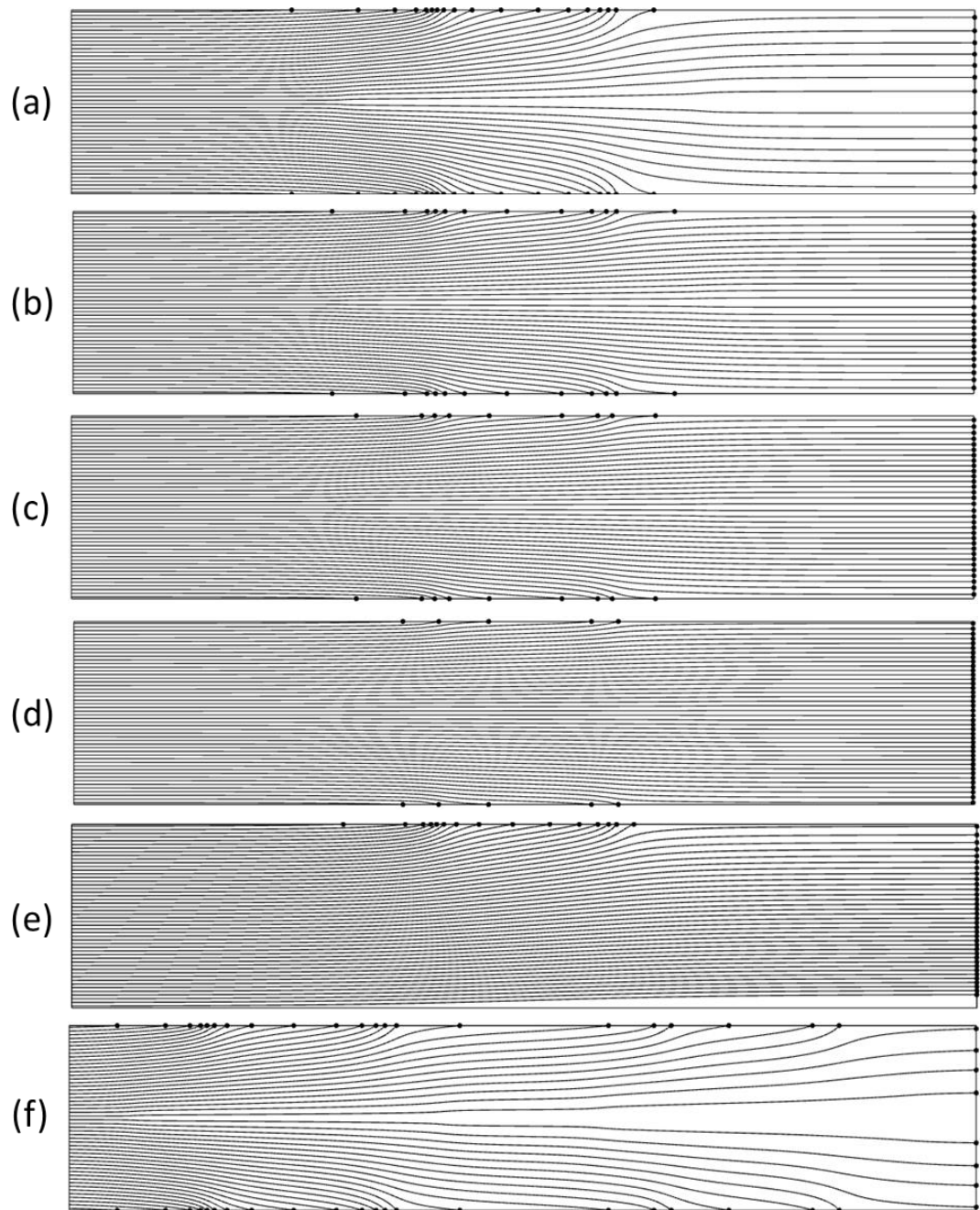
Figure 4.11: Simulation result demonstration: (a) 5 ml/min (single pair magnet), (b) 10 ml/min (single pair magnet), (c) 15 ml/min (single pair magnet), (d) 30 ml/min (single pair magnet), (e) single side magnet arrangement（10 ml/min), (f) dual pair magnet arrangement（10 ml/min)

4.3.1 Effect of Flowrate of the Magnetic Nanoparticles Fractionation Performance

Figure 4.12 show the particle size distribution results of the MNP fractions retained in three separation columns by varying the flowrate of the MNPs feed. According to **Figure 4.13**, the particle size distribution becomes narrower from the first column to the third column. The bell-shaped distribution curve of MNP fractions retained in the third column has the sharpest and narrowest shape as compared to that of the other two columns. On the other hand, the average hydrodynamic size of the MNPs captured and separated in each column by CF-LGMS technique with different feed flowrate is shown in **Figure 4.13.** Based on the results, it can be seen that the differences among the average hydrodynamic sizes of MNP fractions retained in the three columns become smaller when the flowrate of the MNP solution increases. This is because the separation of the size was efficient in the first two columns and particle size fractionation is considered to be effective under this scenario. Under this scenario, the larger particles have been separated from in the first column, and the intermediate particle size separatedbeing segregated in from the second column, whereas the remaining smaller particles is retained in the third column. Additionally, under the slower flowrate, there is a longer residence time for more MNPs to be captured in the first two columns, leading to decline in the concentration of the MNPs inside the fluid following into the third column whichbut mostly are in particles with smaller particle size. So, the simulation of the size fractionation by CF-LGMS with flowrate of 5 mL/min shows a better performance in size fractionation of MNPs which is able to generate MNP fractions with the greater degree of monodispersity of the MNPs system.
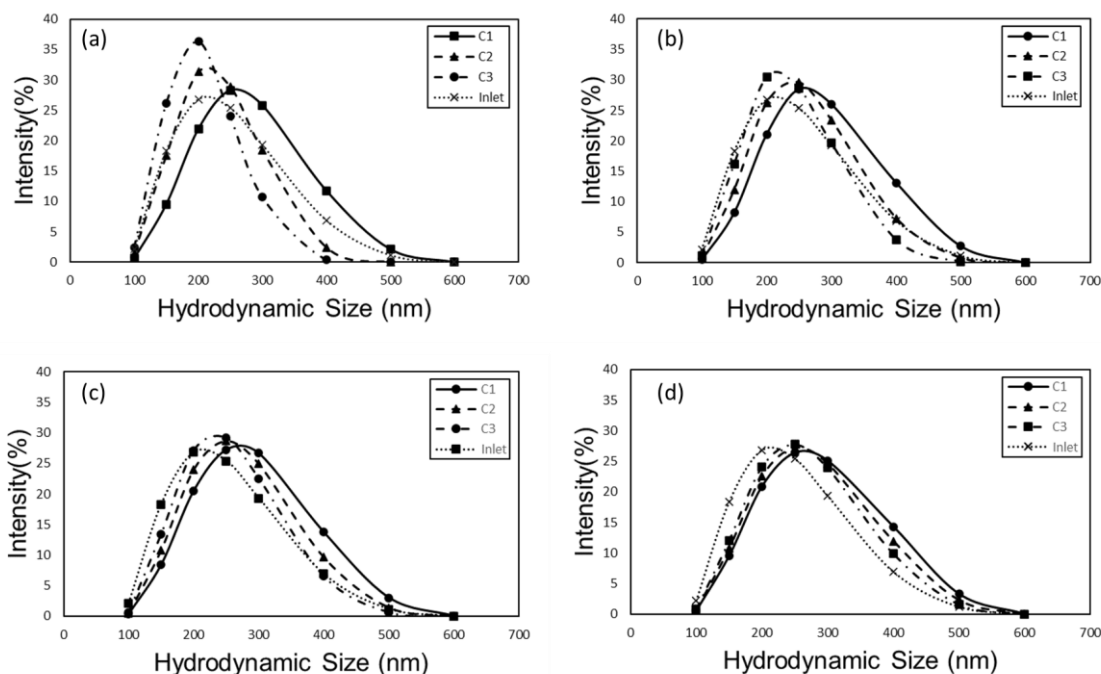
Figure 4.12: Size distribution of MNPs in different columns for CF-LGMS conducted at different flowrate (COMSOL simulation): (a) 5 mL/min, (b) 10 mL/min, (c) 15 mL/min, (d) 30 mL/min
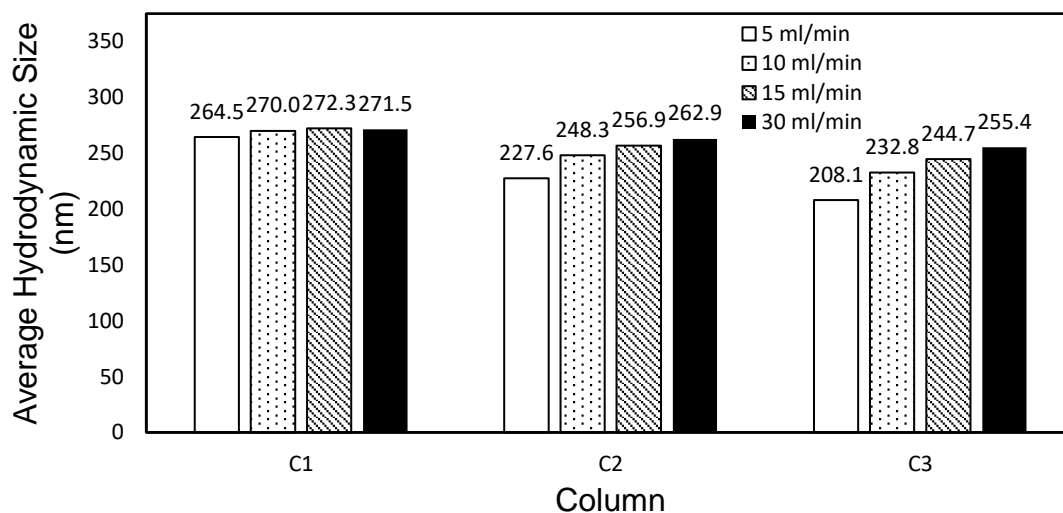

Figure 4.13: Hydrodynamic Size of MNPs in each column for CF-LGMS conducted at different flowrate (COMSOL simulation)

On the other hand, once the flowrate increases, the size distribution of MNP fractions retained in each column become wider and overlap among each other,

especially under the flowrate of 30 mL/min, the difference between the size distribution curves of the different MNP fractions is barely noticeable (**Figure 4.12(d)**). his simulation has proven the theoretical deduction as mentioned above, in which when the flowrate increases, the residence time for the MNPs to remain in the separation columns and subjected to magnetophoresis reduces. Therefore, the size fractionation of MNPs by using CF-LGMS technique will not be that efficient if it is conducted under the higher flowrate. In term of the relationship between flow rate and MNP size fractionation performance, the simulation agrees well with the experimental observations.

4.3.2   Effect of Magnet Arrangement of the Magnetic Nanoparticles Fractionation Performance

The effect of the magnet arrangement on the performance of CF-LGMS in size fractionation of MNPs is also being studied using the computational simulation to further support and explain the experimental result as well as understand the principle behind it. **Figure 4.14** shows size distribution of MNPs in different columns under one side magnet arrangement. The simulation results on the size distribution of MNP fractions produced by the single side as well as the dual pair magnet arrangements show an obvious discrepancy (**Figure 4.14 (b)**). For the MNP fractions resulted from the dual pair magnet arrangement, the size distribution curves show a significant reduction in the range of the particle size as one mores from the upstream towards the downstream. Additionally, the intensity of the peak of the distribution curves also increases, with the peak shifting to the left, for the MNP fractions retained in the first to the third columns. This indicates that the MNP fractions are more concentrated to a specific particle size with narrower size range and the higher degree of monodispersity. On the contrary, after undergoing the size fractionation by CF-LGMS technique under single side magnet arrangement, all the distribution of the three MNP fractions has the similar shape and peak (**Figure 4.14 (a)**). Although this experiment is conducted under the flowrate of 10 mL/min, the single side magnet arrangement has imposed limited

region with intense magnetic field gradient inside the separation column. Due to this fact, the MNP fractionation efficiency by using the CF-LGMS technique decreases.
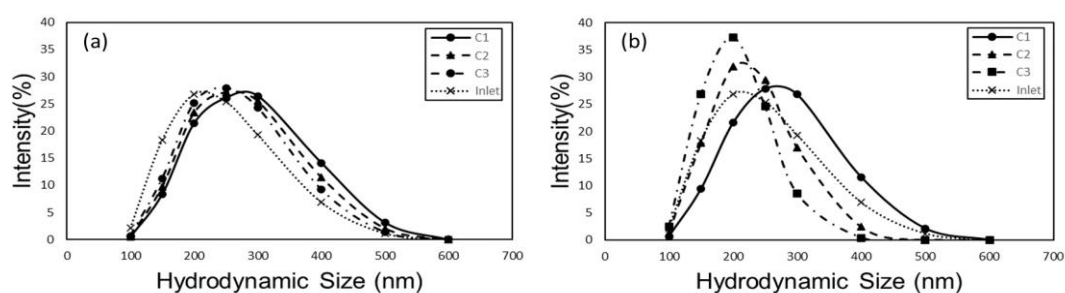

Figure 4.14: Size distribution of MNP fractions in retained in different columns of CF-LGMS system conducted under different magnet arrangement (COMSOL Simulation): (a) single side magnet arrangement, (b) dual pair magnet arrangement

Figure 4.15 shows the average hydrodynamic size of the MNP fractions retained in the three separation columns subjected to CF-LGMS with different magnet arrangement, obtained from the model simulation and theoretical calculation. Based on the simulation results, the average hydrodynamic size for size fractionation by using single side magnet arrangement are 272.53 nm, 262.88 nm and 254.46 nm, for the MNP fractions retained in the first, second and third columns, respectively. Meanwhile, upon subjected to dual pair magnet arrangement, the given MNP fractions have average hydrodynamic size of 264.986 nm, 226.317 nm and 205.784 nm respectively. This simulation result is also showing the similar trend as the experimental results. It is obvious that the difference in average hydrodynamic size for the MNP fractions retained in the three separation columns is more apparent for the CF-LGMS conducted under dual pair magnet arrangement as compared to single side magnet arrangement. As mentioned above, the dual pair magnet arrangement produces the higher proportion of intense magnetic field gradient within the column. Thus, most of the MNPs with larger particle size are separated in the first column, which gives rise to MNP fractions with the higher average hydrodynamic size. Similarly, the intermediate- and tiny-sized MNPs can be separated in the second column and third column respectively, in which the size distribution of these MNP fractions to show the distinct differences. On the

other hand, under the single side magnet arrangement, there is insufficient of intense magnetic field induced in the columns, which is causing some of the larger-sized MNP to be flushed to the downstream column without being captured. Thereby, under this scenario, the average hydrodynamic size of the MNP fractions retained at the downstream columns increased due to the collection of the large particle size which were not being separated in the upstream column.
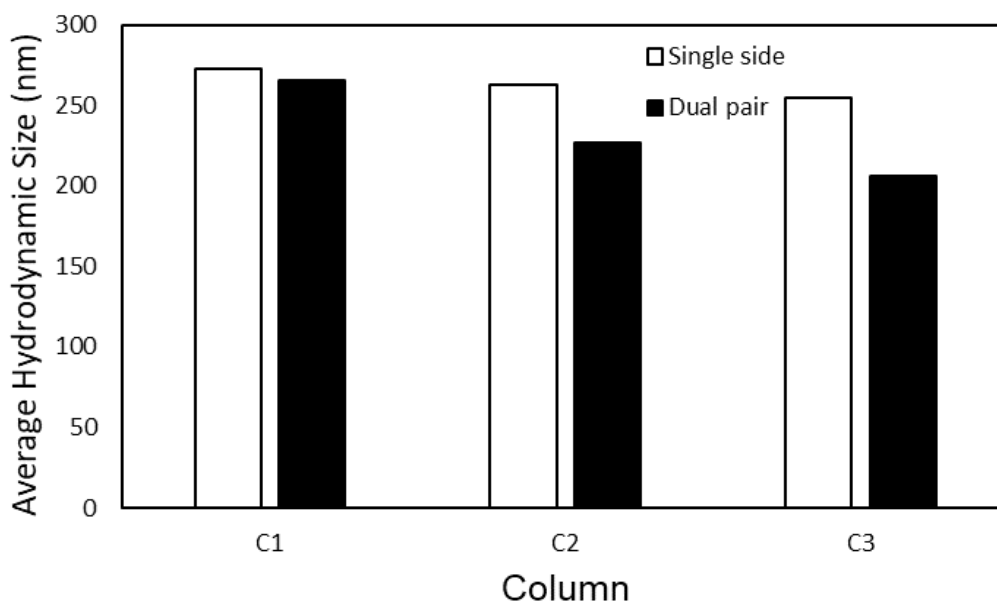

Figure 4.15: Hydrodynamic Size of MNP fractions in retained in different columns of CF-LGMS system conducted under different magnet arrangement (COMSOL simulation)

4.3.3 Separation Efficiency

Last but not least, the separation efficiency of both the experimental and simulation results are compared presented in **Figure 4.16** to evaluate the reliability of the results. The comparison implies that the separation efficiency resulted from both the experiment and simulation is similar, with differences of no more than 5% except for the CF-LGMS by using single side magnet arrangement. Notably, the separation efficiency in the experimental set for the single side magnet arrangement is higher than the simulation outcome, indicating that the actual separation of the MNPs under single side magnet arrangement was more effective than the simulation prediction. The reason of this may be due to simulation of the single side magnet has the lower magnetic field coverage as compared to the reality. However, separation efficiency alone cannot determine the capability of the CF-LGMS to produce monodispersed MNP system. While there are the presence of minor discrepancy, the simulation and experimental results align in terms of size distribution, average hydrodynamic size as well as separation efficiency. Hence, the model used in this simulation is considered an effective tool to depict the size fractionation process by using CF-LGMS technique.
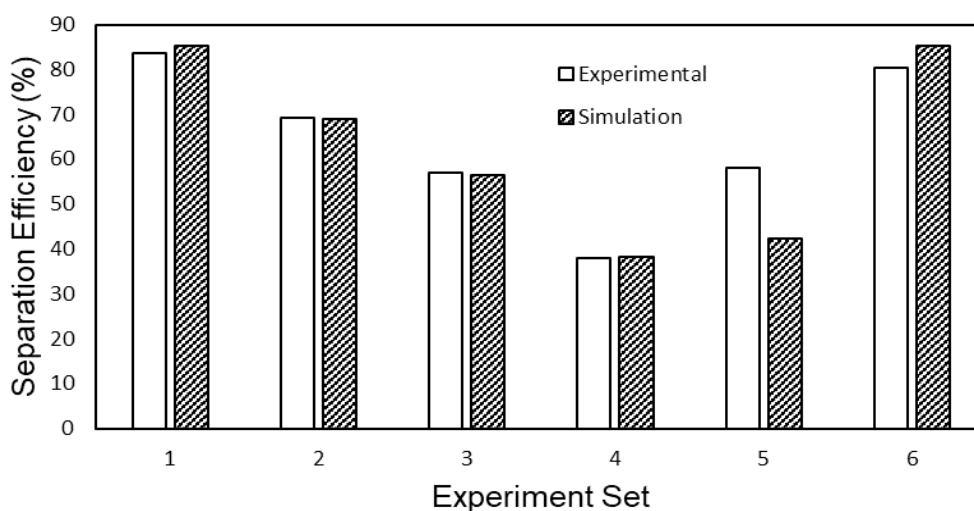

Figure 4.16: Comparison of separation efficiency between experimental and simulation results: (1) 5 ml/min, (2) 10 ml/min, (3) 15 ml/min, (4) 30 ml/min, (5) single side magnet arrangement, (6) dual pair magnet management for different experimental set as shown in Table 3.4 .

CHAPTER 5

CONCLUSION AND RECOMMENDATIONS

5.1   Conclusion

The colloidal instability of bare MNPs leads to reduced effectiveness in many engineering applications, as they tend to agglomerate quickly. To address this issue, functionalization (surface modification) of MNPs with polyelectrolytes is necessary prior to their use in real-time applications. In this study, polyelectrolytes were used to functionalize MNPs, improving their colloidal stability and enabling the two components to bind via physical interactions. The main objective of the research is to identify the optimal functionalization condition that produces the most stable MNP systems.

The experiments showed that modifying the mass ratio of polyelectrolyte (PSS) to MNPs during surface functionalization resulted in MNP systems with varying average particle size and particle size distribution. The experiments revealed that varying the mass ratio of polyelectrolyte (PSS) to MNPs during surface functionalization resulted in MNP systems with different average particle sizes and particle size distributions. Specifically, changing the mass ratio of MNPs to PSS from 1:0.5 to 1:4 led to distinct variations in the generated MNP systems' average particle size and particle size distribution. To identify the most colloidally stable MNPs system, the 1:1 mass ratio of MNPs to PSS was selected. This choice was based on the fact that the resulting MNPs system had the smallest average hydrodynamic size and the narrowest particle size distribution. As the size of MNPs decreases, the likelihood of agglomeration decreases, thereby improving colloidal stability.

In order to produce the MNPs with improved monodispersity, CF-LGMS technique was introduced to perform the separation process. The second objective was to experimentally study the effect of flowrate and magnet configurations on the monodispersity of magnetic nanoparticle systems fractionated by CF-LGMS. The flowrate (single pair magnet arrangement) was altered at 5 ml/min, 10 ml/min, 15 ml/min and 30 ml/min, whereas the magnet arrangement (10 ml/min) was manipulated for single side and dual pair magnets. According to the result, the size distribution curves show a narrowing trend when the flowrate decreased, especially at 5 ml/min. When the flowrate became 30 ml/min, the size distribution curves almost overlapped with each other. Additionally, with the dual pair magnet arrangement, the size distribution curves also show noticeable narrowing results. In the aspect of the average hydrodynamic size, the flowrate of 5 ml/min and the dual pair magnet arrangement experiment sets shows visible drop in the size of MNPs across the separation columns. Furthermore, the average hydrodynamic size of the MNPs separated in the three columns also show noticeable difference: 5 ml/min (244.1 nm, 191.6 nm and 158.2 nm) ; dual pair magnet arrangement (249.6 nm, 200.6 nm and 167.7 nm). Moreover, in terms of monodispersity, these two experiment sets showed a decrement in the standard deviation as well as the PDI values. This signified that the separated MNPs are centralized to the average particle size without wide deviation. The third objective of this study is to develop a mathematical model which is able to describe the fractionation process by using CF-LGMS technique. After conducting the simulation using COMSOL Multiphysics, the simulated results are similar to the experimental results. It is crystal clear that slower flowrate and greater amount of magnets can significantly enhance the size fractionation of the MNPs via CF-LGMS process. Therefore, the dual pair of magnet arrangement together with slow flowrate is preferable to generate a monodispersed MNPs system.

5.2   Recommendation and Improvement

There are several recommendations to improve and further extend this project in the future:

1. It is possible to acquire the SEM and TEM pictures of the polyelectrolyte-functionalized MNPs to directly observe the geometry and structure of the resulting particle systems.

2. The hydrodynamic as well as the cooperative effect can be involved in the analysis of the results in order to study in depth on the separation process using CF-LGMS technique.

3. Modeling design for CF-LGMS model simulation can be in 3-dimensional space to extensively simulate the separation process in the separation columns. In 3-dimensional space, we can further understand the MNPs flow behavior in the separation process.

REFERENCES

Aisida, S., Ahmad, I. and Ezema, F., 2022. Surface functionalization of magnetic nanoparticles: potentials for biomedical applications. Fundamentals and Industrial Applications of Magnetic Nanoparticles, pp.237-253.

Ajinkya, N., Yu, X., Kaithal, P., Luo, H., Somani, P. and Ramakrishna, S., 2020. Magnetic Iron Oxide Nanoparticle (IONP) Synthesis to Applications: Present and Future. Materials, 13(20), p.4644.

Akbarzadeh, A., Samiei, M. and Davaran, S., 2012. Magnetic nanoparticles: preparation, physical properties, and applications in biomedicine. Nanoscale Research Letters, 7(1).

Ansari, S., Ficiarà, E., Ruffinatti, F., Stura, I., Argenziano, M., Abollino, O., Cavalli, R., Guiot, C. and D'Agata, F., 2019. Magnetic Iron Oxide Nanoparticles: Synthesis, Characterization and Functionalization for Biomedical Applications in the Central Nervous System. Materials, 12(3), p.465.

Bhandari, P. (2023) How to calculate standard deviation (guide): Calculator & examples, Scribbr. Available at: https://www.scribbr.com/statistics/standard-deviation/ (Accessed: April 17, 2023).

Chong, P., Tan, Y., Teoh, Y., Lim, C., Toh, P., Lim, J. and Leong, S., 2021. Continuous Flow Low Gradient Magnetophoresis of Magnetic Nanoparticles: Separation Kinetic Modelling and Simulation. Journal of Superconductivity and Novel Magnetism, 34(8), pp.2151-2165.

Clayton, K., Salameh, J., Wereley, S. and Kinzer-Ursem, T., 2016. Physical characterization of nanoparticle size and surface modification using particle scattering diffusometry. Biomicrofluidics, 10(5), p.054107.

Daou, T., Pourroy, G., Bégin-Colin, S., Grenèche, J., Ulhaq-Bouillet, C., Legaré, P., Bernhardt, P., Leuvrey, C. and Rogez, G., 2006. Hydrothermal Synthesis of Monodisperse Magnetite Nanoparticles. Chemistry of Materials, 18(18), pp.4399-4404.

De Las Cuevas, G., Faraudo, J. and Camacho, J., 2008. Low-Gradient Magnetophoresis through Field-Induced Reversible Aggregation. The Journal of Physical Chemistry C, 112(4), pp.945-950.

Deng, H., Li, X., Peng, Q., Wang, X., Chen, J. and Li, Y., 2005. Monodisperse Magnetic Single-Crystal Ferrite Microspheres. Angewandte Chemie International Edition, 44(18), pp.2782-2785.

Faraji, M., Yamini, Y. and Rezaee, M., 2010. Magnetic nanoparticles: Synthesis, stabilization, functionalization, characterization, and applications. Journal of the Iranian Chemical Society, 7(1), pp.1-37.

Faraudo, J., Andreu, J., Calero, C. and Camacho, J., 2016. Predicting the Self-Assembly of Superparamagnetic Colloids under Magnetic Fields. Advanced Functional Materials, 26(22), pp.3837-3858.

Faraudo, J., Andreu, J. and Camacho, J., 2013. Understanding diluted dispersions of superparamagnetic particles under strong magnetic fields: a review of concepts, theory and simulations. Soft Matter, 9(29), p.6654.

Faraudo, J. and Camacho, J., 2009. Cooperative magnetophoresis of superparamagnetic colloids: theoretical aspects. Colloid and Polymer Science, 288(2), pp.207-21

Feng, Q., Liu, Y., Huang, J., Chen, K., Huang, J. and Xiao, K., 2018. Uptake, distribution, clearance, and toxicity of iron oxide nanoparticles with different sizes and coatings. Scientific Reports, 8(1).

Gambhir, R.P., Rohiwal, S.S. and Tiwari, A.P. (2022) "Multifunctional surface functionalized magnetic iron oxide nanoparticles for biomedical applications: A Review," Applied Surface Science Advances, 11, p. 100303

Gatard, V., 2021. Alkaline water electrolysis enhanced by radio frequency alternating magnetic field. [ebook] Available at: <https://tel.archives-ouvertes.fr/tel-03628368/document> [Accessed 20 July 2022].

Gómez-Pastora, J., Bringas, E. and Ortiz, I., 2014. Recent progress and future challenges on the use of high performance magnetic nano-adsorbents in environmental applications. Chemical Engineering Journal, 256, pp.187-204.

Hayes, A., 2022. What Is a Confidence Interval?. [online] Investopedia. Available at: <https://www.investopedia.com/terms/c/confidenceinterval.asp> [Accessed 7 September 2022].

Hinge, N., Pandey, M., Singhvi, G., Gupta, G., Mehta, M., Satija, S., Gulati, M., Dureja, H. and Dua, K., 2020. Nanomedicine advances in cancer therapy. Advanced 3D-Printed Systems and Nanosystems for Drug Delivery and Tissue Engineering, pp.219-253.

Kang, Y., Risbud, S., Rabolt, J. and Stroeve, P., 1996. Synthesis and Characterization of Nanometer-Size Fe3O4 and γ-Fe2O3 Particles. Chemistry of Materials, 8(9), pp.2209-2211.

Khan, I., Saeed, K. and Khan, I., 2019. Nanoparticles: Properties, applications and toxicities. Arabian Journal of Chemistry, 12(7), pp.908-931.

Koo, K., Ismail, A., Othman, M., Bidin, N. and A Rahman, M., 2019. Preparation and characterization of superparamagnetic magnetite (Fe3O4) nanoparticles: A short review. Malaysian Journal of Fundamental and Applied Sciences, 15(1), pp.23-31.

Leong, S., Ahmad, Z., Camacho, J., Faraudo, J. and Lim, J., 2017. Kinetics of Low Field Gradient Magnetophoresis in the Presence of Magnetically Induced Convection. The Journal of Physical Chemistry C, 121(9), pp.5389-5407

Leong, S., Ahmad, Z., Low, S., Camacho, J., Faraudo, J. and Lim, J., 2020. Unified View of Magnetic Nanoparticle Separation under Magnetophoresis. Langmuir, 36(28), pp.8033-8055.

Leong, S., Yeap, S. and Lim, J., 2016. Working principle and application of magnetic separation for biomedical diagnostic at high- and low-field gradients. Interface Focus, 6(6), p.20160048.

Leong, S.S., Ahmad, Z. and Lim, J.K. (2015) "Magnetophoresis of superparamagnetic nanoparticles at low field gradient: Hydrodynamic effect," Soft Matter, 11(35), pp. 6968–6980.

Li, X., Li, W., Wang, M. and Liao, Z., 2021. Magnetic nanoparticles for cancer theranostics: Advances and prospects. Journal of Controlled Release, 335, pp.437-448.

Lim, J., Yeap, S. and Low, S., 2014. Challenges associated to magnetic separation of nanomaterials at low field gradient. Separation and Purification Technology, 123, pp.171-174.

Lu, A., Salabas, E. and Schüth, F., 2007. Magnetic Nanoparticles: Synthesis, Protection, Functionalization, and Application. Angewandte Chemie International Edition, 46(8), pp.1222-1244.

Moeser, G., Roach, K., Green, W., Alan Hatton, T. and Laibinis, P., 2004. High-gradient magnetic separation of coated magnetic nanoparticles. AIChE Journal, 50(11), pp.2835-2848.

Nlm.nih.gov. 2022. Standard Deviation. [online] Available at: <https://www.nlm.nih.gov/nichsr/stats_tutorial/section2/mod8_sd.html> [Accessed 29 August 2022].

Raja, P.M.V. and Barron, A.R. (2022) 2.4: Dynamic light scattering, Chemistry LibreTexts. Libretexts. Available at: https://chem.libretexts.org/Bookshelves/Analytical_Chemistry/Physical_Methods_in_Chemistry_and_Nano_Science_(Barron)/02%3A_Physical_and_Thermal_Analysis/2.04%3A_Dynamic_Light_Scattering (Accessed: April 24, 2023).

Raval, N., Maheshwari, R., Kalyane, D., Youngren-Ortiz, S., Chougule, M. and Tekade, R., 2019. Importance of Physicochemical Characterization of Nanoparticles in Pharmaceutical Product Development. Basic Fundamentals of Drug Delivery, pp.369-400.

Sadeghi, R. et al. (2014) "Investigation of alumina nanofluid stability by UV–vis spectrum," Microfluidics and Nanofluidics, 18(5-6), pp. 1023–1030.

Salvador, M. et al. (2021) "Microemulsion synthesis of superparamagnetic nanoparticles for Bioapplications," International Journal of Molecular Sciences, 22(1), p. 427.

Shaw, S., Shit, G. and Tripathi, D., 2022. Impact of drug carrier shape, size, porosity and blood rheology on magnetic nanoparticle-based drug delivery in a microvessel. Colloids and Surfaces A: Physicochemical and Engineering Aspects, 639, p.128370.

Software for simulating static and low-frequency electromagnetics (no date) COMSOL. Available at: https://www.comsol.com/acdc-module (Accessed: April 24, 2023).

Stetefeld, J., McKenna, S.A. and Patel, T.R. (2016) "Dynamic light scattering: A practical guide and applications in biomedical sciences," Biophysical Reviews, 8(4), pp. 409–427.

Sun, S. and Zeng, H., 2002. Size-Controlled Synthesis of Magnetite Nanoparticles. Journal of the American Chemical Society, 124(28), pp.8204-8205.

Tan, Y.W. et al. (2022) "Low-gradient magnetic separation of magnetic nanoparticles under continuous flow: Experimental Study, Transport Mechanism and Mathematical Modelling," ELECTROPHORESIS, 43(21-22), pp. 2234–2249.

Tartaj, P., Morales, M., Gonzalez-Carreño, T., Veintemillas-Verdaguer, S., Bomati-Miguel, O., Roca, A., Costo, R. and Serna, C., 2016. Biomedical Applications of Magnetic Nanoparticles. Reference Module in Materials Science and Materials Engineering,.

Track charged particles and particles in fluid flow with simulation (no date) COMSOL. Available at: https://www.comsol.com/particle-tracing-module#:~:text=Particle%20tracing%20is%20a%20numerical,rather%20than%20a%20continuous%20field (Accessed: April 24, 2023).

Toh, P., Yeap, S., Kong, L., Ng, B., Chan, D., Ahmad, A. and Lim, J., 2012. Magnetophoretic removal of microalgae from fishpond water: Feasibility of high gradient and low gradient magnetic separation. Chemical Engineering Journal, 211-212, pp.22-30.

Vidal-Vidal, J., Rivas, J. and López-Quintela, M., 2006. Synthesis of monodisperse maghemite nanoparticles by the microemulsion method. Colloids and Surfaces A: Physicochemical and Engineering Aspects, 288(1-3), pp.44-51.

Wang, B., Wei, Q. and Qu, S., 2013. Synthesis and Characterization of Uniform and Crystalline Magnetite Nanoparticles via Oxidation-precipitation and Modified co-precipitation Methods. International Journal of ELECTROCHEMICAL SCIENCE, [online] 8(3), pp.3786-3793. Available at: <http://www.electrochemsci.org/papers/vol8/80303786.pdf> [Accessed 7 August 2022].

Wechsler, S., 1997. Statistics at Square One. Ninth Edition, revised by M. J. Campbell, T. D. V. Swinscow, BMJ Publ. Group, London, 1996. No. of pages: 140. Price: £11. ISBN 0-7279-0916-9. Statistics in Medicine, 16(22), pp.2629-2630.

Xu, C. and Sun, S., 2007. Monodisperse magnetic nanoparticles for biomedical applications. Polymer International, 56(7), pp.821-826.

Yavuz, C., Mayo, J., Yu, W., Prakash, A., Falkner, J., Yean, S., Cong, L., Shipley, H., Kan, A., Tomson, M., Natelson, D. and Colvin, V., 2006. Low-Field Magnetic Separation of Monodisperse Fe3O4 Nanocrystals. Science, 314(5801), pp.964-967.

Yeap, S., Leong, S., Ahmad, A., Ooi, B. and Lim, J., 2014. On Size Fractionation of Iron Oxide Nanoclusters by Low Magnetic Field Gradient. The Journal of Physical Chemistry C, 118(41), pp.24042-24054.

Zahid, M., Nadeem, N., Hanif, M., Bhatti, I., Bhatti, H. and Mustafa, G., 2019. Metal Ferrites and Their Graphene-Based Nanocomposites: Synthesis, Characterization, and Applications in Wastewater Treatment. Nanotechnology in the Life Sciences, pp.181-212.

Zirak, M. et al. (2017) "Carboxymethyl cellulose coated Fe3O4@SiO2 core–shell magnetic nanoparticles for methylene blue removal: Equilibrium, kinetic, and thermodynamic studies," Cellulose, 25(1), pp. 503–515.